



IMAGE: A MAP OF THE STARS OF THE ORION CONSTELLATION

Print ISSN: 2631-8490 Online ISSN: 2631-8504

JournalPreview

London Journal of Research in Science: Natural and Formal
Volume 23 | Issue 9 | Compilation 1.0



JournalPreview

LONDON JOURNALS OF RESEARCH IN SCIENCE: NATURAL AND FORMAL

This document is a pre-published view of London Journal of Research in Science: Natural and Formal Volume 23, Issue 9 and Compilation 1.0. For any minor changes and updations kindly follow your paper's live editing URL given in sent email or get in touch with our support team at support@journalspress.com or visit our website to use live chat support. This is a beta document thus order, content or existence of papers may alter in the published eJournal. You are requested to kindly acknowledge and approve your research paper in this JournalPreview within three days.

Journal Content

In this Issue



- i. Journal introduction and copyrights
- ii. Featured blogs and online content
- iii. Journal content
- iv. Editorial Board Members

-
- 1. A Liebig's Principle of Limiting Factors based Single-Species Population Growth Model I: Qualitative Study of Trajectories and Fitting Results. **1-23**
 - 2. Structural and Dielectric Studies of Ni doped TiO₂ Thin Films for Electro-Optic Devices. **25-32**
 - 3. Etiological Aspects of Fusarium Corn Stalk Rot Under the Cold Tropic Conditions. **33-50**
 - 4. Content Analysis of Design Language based on User Evaluation and Experience. **51-59**

-
- V. Great Britain Journals Press Membership



Scan to know paper details and
author's profile

A Liebig's Principle of Limiting Factors based Single-Species Population Growth Model I: Qualitative Study of Trajectories and Fitting Results

*Héctor A. Echavarría-Heras, Cecilia Leal-Ramírez, Omar Valencia Méndez
& Elia Montiel-Arzate*

ABSTRACT

In this contribution, we propose a single-species population growth model formulated using ideas emanating from Liebig's principle of limiting factors. The inherent natural natality rate determines by the minimum between the size of the population and that of a resource on which the population depends for sustenance. Moreover, emulating the unrestricted population growth assumption, we hypothesise that the associating natural mortality rate is proportional to population size. We also consider that the external feeding resource's consumption rate varies directly proportional to the natural growth rate of the population. In this delivery, we present a qualitative study of the associated trajectories and fitting results based on data on populations growing under experimental or natural conditions. The possible phase configurations include regimes with stable equilibria, sigmoidal growth, extinction, or stationarity. All study cases confirmed that the offered model entails high reproducibility of observed variation patterns while supplying remarkable interpretative capabilities. The proposed model also allows simultaneous identification of the population size trajectory and the resource abatement function.

Keywords: liebig's principle of limiting factors, single-species population growth model.

Classification: LCC: QA

Language: English



Great Britain
Journals Press

LJP Copyright ID: 925691

Print ISSN: 2631-8490

Online ISSN: 2631-8504

London Journal of Research in Science: Natural and Formal

Volume 23 | Issue 9 | Compilation 1.0



© 2023, Héctor A. Echavarría-Heras, Cecilia Leal-Ramírez, Omar Valencia Méndez & Elia Montiel-Arzate. This is a research/review paper, distributed under the terms of the Creative Commons Attribution-Noncommercial 4.0 Unported License <http://creativecommons.org/licenses/by-nc/4.0/>, permitting all noncommercial use, distribution, and reproduction in any medium, provided the original work is properly cited.

A Liebig's Principle of Limiting Factors based Single-Species Population Growth Model I: Qualitative Study of Trajectories and Fitting Results

Héctor A. Echavarría-Heras^a, Cecilia Leal-Ramírez^o, Omar Valencia Méndez^p
& Elia Montiel-Arzate^o

ABSTRACT

In this contribution, we propose a single-species population growth model formulated using ideas emanating from Liebig's principle of limiting factors. The inherent natural natality rate determines by the minimum between the size of the population and that of a resource on which the population depends for sustenance. Moreover, emulating the unrestricted population growth assumption, we hypothesise that the associating natural mortality rate is proportional to population size. We also consider that the external feeding resource's consumption rate varies directly proportional to the natural growth rate of the population. In this delivery, we present a qualitative study of the associated trajectories and fitting results based on data on populations growing under experimental or natural conditions. The possible phase configurations include regimes with stable equilibria, sigmoidal growth, extinction, or stationarity. All study cases confirmed that the offered model entails high reproducibility of observed variation patterns while supplying remarkable interpretative capabilities. The proposed model also allows simultaneous identification of the population size trajectory and the resource abatement function. One phase of Liebig's limiting factors principle-driven model can consistently mimic population size abatement to extinction. Such a feature misses improved in regularly conceived S-shaped population growth models.

Keywords: liebig's principle of limiting factors, single-species population growth model.

Author α σ ρ : Centro de Investigación Científica y de Estudios Superiores de Ensenada, Carretera Ensenada-Tijuana No. 3918, Zona Playitas, Código Postal 22860, Apdo. Postal 360 Ensenada, B.C. México.

o: Instituto Tecnológico de México, boulevard Tecnológico #150, Ex Ejido Chapultepec, C.P. 22780, Ensenada B.C, México.

I. INTRODUCTION

The optimal settings for biological processes often occur at the minimum and maximum values of relevant variables (Ghaleb et al., 2020; Peeters & Gardeniers, 1998). The concept of extreme value control ascended from results reported by K. Sprengel in 1839 (Sprengel, 1839; El-Sharkawy, 2011) and later popularised by Justus von Liebig, stating that the nutrient present in the minimum determines the rate of growth of a particular organism (Liebig, 1843). This observation led to the establishment of Liebig's Principle of Limiting Factors, also known as Liebig's Law of the Minimum (Rizhinashvili, 2022; Anees, 2022). Agents that slow down growth in an ecosystem constitute limiting factors. Control exerts by either the minimum or maximum values that the factor can assume over a gradient of variation. Based on lower and upper tolerance limits, Liebig's Law of the Minimum was generalised into the Law of the Tolerance of

Shelford (Shelford, 1913). Furthermore, limiting factors can indirectly influence the impact of other non-limiting factors by interacting with them. This principle, known as the principle of Limiting Factors, is treasured in studying the entire or parts of ecosystems (Odum,1963; Odum,1971).

Although in the ecological literature, the control by extreme values regularly cites, its utilisation as a conceptual framework for population growth models is limited. The initial effort to apply this concept was due to I. A. Polyetayev et al. in 1971, who proposed a Liebig's Principle of Limiting Factors-based model for predator-prey interactions (Polyetayev et al., 1971). In the Polyetayev model, the natality rate for the prey population determines by the minimum between the population size and the extent of an external resource representing feeding energy availability. Building upon these ideas, Echavarría and Gomez (1979) and Montiel-Arzate, et al. (2004) further developed related population models by maintaining natality as controlled by Liebig's Law of the Minimum but emulating Shelford's Law of Tolerance by hypothesising that the mortality rate regulates by the maximum value of factors depending on population size. Recently, Echavarría-Heras et al. (2021) revised the approach by Montiel-Arzate et al. (2004) to propose a model for the growth of a single species population built upon the Liebig-Shelford as mentioned earlier paradigm for the control of the related natural growth rate, but including a specific scaling or weighting of population size to model the increase in mortality promoted by low population densities. This last approach reported consistent reproducibility when fitted on real data sets. However, the authors also reported inconveniences since a direct fitting procedure that relies on estimates' initial values brought high sensibility associated with local minimum problems at the nonlinear acquisition of final values. Therefore, a revision aimed to avoid or at least lessen the parameter estimation burden experienced deems necessary. In that vein, reducing the complexity associated with the Echavarría-Heras et al. (2021) construct while simultaneously keeping its reproducibility strength endures a reasonable rationale. For that aim, in this contribution, we modify the protocol by Echavarría-Heras et al. (2021) and propose a single species population growth model, built upon Liebig's Principle of Limiting Factors and such that: (1) the inherent natural natality rate is determined according to Liebig's Law by the minimum between the size of the population and that of the resource on which the population depends for sustenance, (2) by partially emulating the unrestricted population growth hypothesis the add-on natural mortality rate is supposed to be proportional solely to population size, and (3) the rate of consumption of the external feeding resource ostensibly varies directly proportional to the natural growth rate of the population. The resulting model identifies further as Liebig's Principle of Limiting Factors Population Growth Model or Liebig's Law Population Model (LLPM). Despite being partially founded on the assumption that mortality depends linearly on population size, the present model demonstrated a proven capability to mimic the typical s-shaped pattern associated with restricted growth models—besides, a lesser complexity demonstrated to be advantageous in finding parameter estimates for consistent reproducibility. We include several examples based on observed data that confirm the empirical and interpretative adequacy of the present paradigm. An appendix presents the formalities behind a qualitative study of the associating global trajectory.

II. THEORETICAL APPROACH

For present aims, we denote through $x(t)$ a quantitative measure of the size of a single-species population at a time t . It could be understood by $x(t)$, for example, the biomass of all animals composing the population, or their number, if it is suitably large and changes continuously. We additionally assume that the maintenance of the population depends on the presence of an external resource or agent whose extent at time t denotes using $R(t)$. For instance, $R(t)$ could

stand for: the food solution for a culture of bacteria; the amount of solar energy with which the primary producers photosynthetically elaborate carbohydrates; the biomass of autotrophs upon which herbivores fed or the biomass of these later that provide nourishment for carnivores; the pool of antibiotics that limit the proliferation of a bacterial population; the number of nests available for a bird species.

We now explain how Liebig’s Law of the Minimum statement can produce a population growth model under a limiting resource. For that aim, we use the symbol $\dot{x}(t)$ to denote the natural growth rate of population size $x(t)$ at a time t . Formally, the proposed model states that

$$\dot{x}(t) = f(R(t), x(t))x(t) \tag{1}$$

where $R(t)$ at time t stands for the amount of a resource that the population requires to stand by, and $f(R(t), x(t))$ is a function depending on both $x(t)$ and $R(t)$ and represents the intrinsic population growth rate at a time t . Along Equation (1), we take on the initial conditions $R_0 = R(0)$, and $x_0 = x(0)$.

Following Charlebois and Balázsi (2018) and Echavarría-Heras et al. (2021), we assume that the natural population growth rate and resource consumption relate such that

$$\frac{dR(t)}{dt} = -p \frac{dx(t)}{dt} \tag{2}$$

where p is a positive constant. Integration yields

$$R(t) = R_0 - p(x(t) - x_0) \tag{3}$$

In order to provide a representation of Equation (1) deriving from Liebig’s Law of the Minimum, we assume that at a given time, t population size $x(t)$ sets by the balance of two opposite processes: one having intensity $N(t)$ and nourishing the number of births, and another of a strength $M(t)$ inducing the natural death of individuals in the population.

This work will limit ourselves to where $R(t)$ stands for the population’s external energy source. To facilitate the reasoning, we will assume that $R(t)$ and $x(t)$ at each time t can be measured with the same units and compare them directly. $R(t)$ might be such that, at time t , satisfies the essential needs of all population individuals. For example, if each individual of a herbivorous population consumes an average of p kg of food at time t , then an energy source of value $p x(t)$ could satisfy the vital needs of the population. In other words, if the number of individuals $x(t)$ is less than the magnitude of the energy source $R(t)$ at time t , then there will be no lack of food for the population, and we could assume that the intensity of the birth process $N(t)$ depends on the number of individuals $x(t)$ at each instant t . If, on the contrary, $x(t)$ is more significant than $R(t)$, then only some individuals equal to $R(t)$ at time t will be able to feed normally and the intensity of the birth process $N(t)$ will set by $R(t)$ for each t . In summary, considering Liebig’s Law of the Minimum, we may consider a positive constant a , such that

$$N(t) = a \min_t \{x(t), R(t)\} \tag{4}$$

The minimum operation extends to all values of t considered in a specific interval, say of the type $[0, T]$, where T can be any real number.

Correspondingly, we will assume that the intensity of the natural death process $M(t)$ sets is directly proportional to the number of individuals in the population. That is, for b , a positive constant, we take

$$M(t) = bx(t) \tag{5}$$

Then, the natural population growth rate $x(t)$ is formally given by the balance of $N(t)$ and $M(t)$,

$$\dot{x}(t) = N(t) - M(t) \tag{6}$$

Combining Equations (4) through (6) the intrinsic population growth rate $f(R(t), x(t))$ introduced in Equation (1), takes the form,

$$f(R(t), x(t)) = a \min(x(t), R(t))/x(t) - b \tag{7}$$

Therefore, Equation (1) gets the piece wisely defined form

$$\dot{x}(t) = \begin{cases} (a - b)x(t) & \text{for } x(t) \leq R(t) \\ aR(t) - bx(t) & \text{for } x(t) > R(t) \end{cases} \tag{8}$$

Moreover, replacing $R(t)$ as given by Equation (3) into Equation (8) and simplifying leads to

$$\dot{x}(t) = \begin{cases} (a - b)x(t) & \text{for } x(t) \leq E \\ (ap + b)(K - x(t)) & \text{for } x(t) > E \end{cases} \tag{9}$$

where

$$E = (R_0 + px_0)/(1 + p) \tag{10}$$

and

$$K = aE(p + 1)(ap + b)^{-1} \tag{11}$$

Note that the expressions of the second member of (9) are continuous functions by virtue that we can suppose that $x(t)$ as much as $R(t)$ are continuous functions of time. The first of the differential equations of (9) is a homogeneous linear equation whose solution is immediate, and the second of these equations is a non-homogeneous linear equation which using an integration factor or via the parameter variation method, can also be solved. Then, the solution $x(t)$ to Equation (9) will be

$$x(t) = \begin{cases} x_1(t) & \text{for } x(t) \leq E \\ x_2(t) & \text{for } x(t) > E \end{cases} \tag{12}$$

where

$$x_1(t) = x_{10}e^{(a-b)t} \tag{13}$$

and

$$x_2(t) = x_{20}e^{-(ap+b)t} + K(1 - e^{-(ap+b)t}) \tag{14}$$

with E and K given by Equations (10) and (11) one to one, x_{10} and x_{20} determined from the requirement that $x(0) = x_0$, and the continuity condition $x_1(t_c) = x_2(t_c)$ being t_c a time value

such that $x(t_c) = E$. Note also that according to equations (9) and (12), $x_1(t)$ will be increasing whenever $a > b$, and conversely, $x_1(t)$ will decrease provided $a < b$ holds. In turn, by Equations (9) and (12), $x_2(t)$ satisfies $\frac{dx_2(t)}{dt} > 0$ whenever the inequality $x_2(t) < K$ holds. In turn, $\frac{dx_2(t)}{dt} < 0$ if $x_2(t) > K$.

Setting $p = 0$ in Equation (3) considers the case where $R(t)$ remains steady at a level R_0 . Equations (10) and (11) become $E = R_0$ and $K = \frac{aR_0}{b}$, one-to-one. Let $x_s(t)$, satisfying $x_s(0) = x_{s0}$, stand for the global trajectory associated with such a stationary case. Then, correspondingly, Equation (9) takes the form

$$\frac{dx_s}{dt} = \begin{cases} (a - b)x_s(t) & \text{for } x_s(t) \leq R_0 \\ aR_0 - bx_s(t) & \text{for } x_s(t) > R_0 \end{cases} \quad (15)$$

And in turn, $x_s(t)$ the stationary form of Equation (12) becomes

$$x_s(t) = \begin{cases} x_{s1}(t) & \text{for } x(t) \leq R_0 \\ x_{s2}(t) & \text{for } x(t) > R_0 \end{cases} \quad (16)$$

where

$$x_{s1}(t) = x_{s10}e^{(a-b)t} \quad (17)$$

$$x_{s2}(t) = x_{s20}e^{-bt} + \frac{aR_0}{b}(1 - e^{-bt}) \quad (18)$$

where, as we have specified around Equation (14), x_{s10} and x_{s20} are integration constants to be determined using the initial condition $x_s(0) = x_{s0}$ and the continuity requirement $x_{s1}(t_c) = x_{s2}(t_c)$ being t_c a time value such that $x_s(t_c) = R_0$.

The stationary characterisation $x_s(t)$ of Equation (12) provides a resource availability model for autotrophic organisms, including photosynthetic bacteria, algae, and plants, that rely on a consistent energy source to withstand their growth and population sustainability. These organisms possess the ability to produce their food through photosynthesis, which entails the transformation of sunlight into chemical energy. As long as there is a stable availability of sunlight, the autotrophic population can thrive and grow. Another instance of a population dependent on a steady energy source is a group of chemosynthetic organisms inhabiting environments with a continuous supply of chemical compounds, such as sulfur or methane. They can generate sustenance using the energy derived from these compounds to support growth and reproduction. In addition, certain heterotrophic populations, such as specific kinds of fungi, can subsist and multiply on a steady energy supply sourced from decomposing organic matter given a constant supply.

The logistic model proposed initially by Verhulst (1838) as a way of modelling population growth under limited availability of resources formally represents employing the differential Equation

$$\dot{x}(t) = ax(t)(1 - x(t)/K) \quad (19)$$

where $x(t)$ stands for population size or density at time t , a is the associated intrinsic rate of increase, and K is a positive constant known as the environmental carrying capacity. The logistic model will provide a reference to assess the reproducibility strength of the global trajectory of Liebig's Principle of limiting factors model of Equation (9).

III. RESULTS

3.1 Qualitative study of the global trajectory $x(t)$

As shown in the appendix, if we have that $a - b < 0$, then for $x_0 \leq E$, the global trajectory $x(t)$ acquires the $x_1(t)$ form given by Equation (13) with $x_{10} = x_0$. Therefore, $x(t)$ is monotonically decreasing for all $t \geq 0$. Because of this, the population size vanishes according to an exponential law. Alternatively, if $a < b$ and $x_0 > E$, $x(t)$ will initially conform to the $x_2(t)$ branch given by Equation (14), setting $x_{20} = x_0$. Since $a < b$ implies $K < E$, we have $\frac{dx_2(t)}{dt} < 0$ and $x_2(t)$ asymptotically approaching the value K . But, by continuity on its descent towards K , there necessarily will be a time t_c such that $x_2(t_c) = E$. Afterwards, the $x(t)$ dynamics will follow the $x_1(t)$ split, which because of the ordering $a < b$, will drive population size to vanish. We can summarise that maintenance of the condition $a < b$ implies the disappearance of the population, regardless of its initial value x_0 (also regardless of whether this value is greater or equal or less than E , see Figure 1).

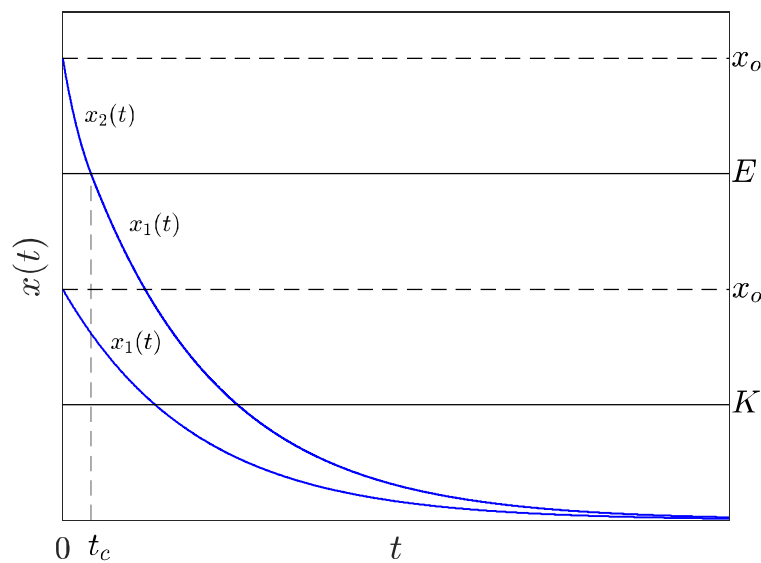


Figure 1: The behaviour of the trajectory $x(t)$ for $a < b$. For $x_0 \leq E$, population size $x(t)$ vanishes, following an exponential law, provided that $a < b$. Whenever $a < b$ and $x_0 > E$, population size $x(t)$ decreases initially according to the $x_2(t)$ correspondence rule approaching the asymptotic value K , which lies below E , when crossing this threshold, the trajectory $x(t)$ ceases to behave according to the rule $x_2(t)$ and switches to the $x_1(t)$ path, and therefore, asymptotically approaching zero as t progresses to infinity.

Consider now the $a > b$ order. Then, we will also have $K > E$. Then, for $x_0 \leq E$, at the beginning of the growth process, population size will describe according to the exponentially increasing path $x_1(t)$. Furthermore, since $x_0 \leq E$ by continuity, there will be a time t_c such that $x_1(t_c) = E$. Afterwards, the $x(t)$ dynamics will switch to being modelled by the $x_2(t)$ stem. Therefore, as the appendix explains, population size $x(t)$ will keep increasing and asymptotically approaching $K > E$. The case $a > b$ and $E < x_0 < K$ portraits similarly with $x(t)$ behaving as the $x_2(t)$ branch and asymptotically approaching K . Besides, whenever $a > b$ and $x_0 > K > E$, the population size $x(t)$ will be described by $x_2(t)$, so the condition $x_0 > K$ will fix $x(t)$ to be decreasing and asymptotically approaching K as t progresses to infinity (Figure 2).

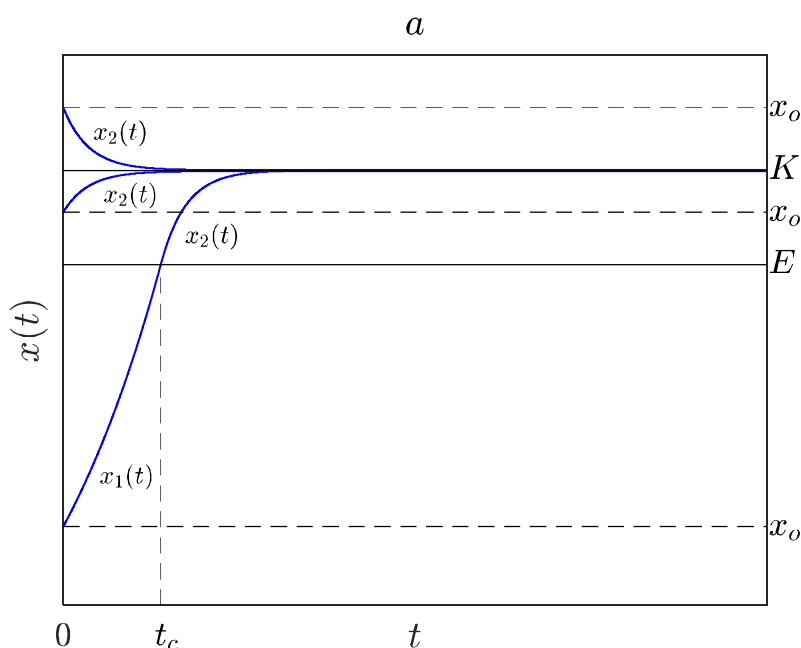


Figure 2: The behaviour of the $x(t)$ trajectory for $a > b$. For $a > b$ and $x_0 \leq E < K$, at the beginning of the process, population size $x(t)$ increases according to the $x_1(t)$ branch; because of continuity, $x_1(t)$ will reach the E threshold at a time t_c . For $t \geq t_c$, population size will keep growing according to $x_2(t)$, thereby asymptotically approaching level K . The case $a > b$ and $E < x_0 < K$ renders similarly with $x(t)$ behaving as the $x_2(t)$ branch approaching K . For $a > b$ and $x_0 > K$, the trajectory decreases from x_0 and approaches the equilibrium level K .

For $a = b$ and the $x_0 \leq E$ ordering, population size $x(t)$ determines by $x_1(t)$, so it remains stationary at x_0 . Assuming that the arrangement $a = b$ and $x_0 > E$ holds, at the start of the growing process, the $x(t)$ trajectory will be determined by the $x_2(t)$ rule with the initial condition $x_{20} = x_0$. As the appendix explains, we also have $\frac{dx_2(t)}{dt} < 0$ for this parameter arrangement so the $x(t)$ trajectory shall decrease and asymptotically approach E .

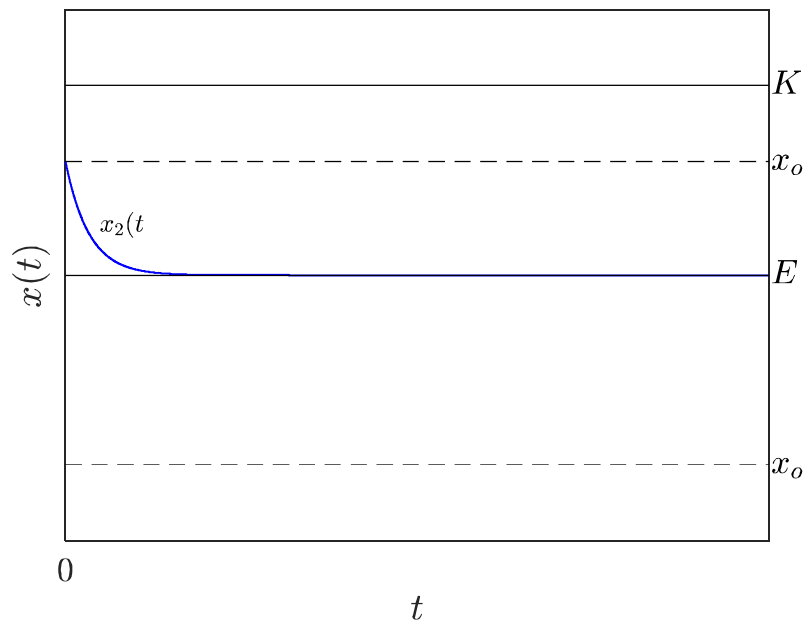


Figure 3: The behaviour of the $x(t)$ trajectory for $a = b$. For $x_0 \leq E$ and $a = b$, the $x(t)$ trajectory remains stationary. For $a = b$ and $x_0 > E$, the trajectory $x(t)$ decreases and asymptotically approaches E .

In summary, the case $a = b$ entitles a heterogeneous behaviour because if the magnitude of the initial population satisfies $x_0 < E$, then population size $x(t)$ remains steady. However, if the initial population size lies above the E threshold, i.e. $x_0 > E$, then $x(t)$ decreases and asymptotically approaches the E threshold (Figure 3).

3.2 Fitting Results

In what follows, we explain the performance of LLPM, Liebig's law population model of Equation (9), as an exploratory tool given different data sets. We address data on yeast grown under ideal conditions in a test tube and the growth of a harbour seal population, both reported by Avissar et al. (2013). We also consider data reported by R. Pearl on the growth of *Drosophila melanogaster* (Pearl, 1927) and data reported by Hughes and Tanner (2000) on the slow decline of an *Agaricia agaricites* population on Jamaican reefs. Fitted parameters, associating standard deviations and Concordance Correlation Coefficient (CCC) values, also denoted utilising the ρ symbol (Lin, 1989), appear in Table 1. To compare the reproducibility strength of offered LLPM, we include CCC values of fits of the logistic model of Equation (19) performed on the included data sets.

Table 1: Estimated values of initial population and resource sizes x_0 and R_0 , as well as parameter, values a, b, p and E produced by fitting the LLPM of Equation (9) to the listed data sets (Avisar et al., 2013; Pearl, 1927; Hughes & Tanner, 2000). Concordance Correlation Coefficient (ρ) values are also displayed.

Data set	x_0	a	b	E	R_0	K	p	ρ_{LLPM}	ρ_{LOG}
Yeast	1.1	0.2549	0.0452	5.7925	8.1388	12.827	0.5	99.23%	98.19%
Seal	1634.24	0.3142	0.1748	4345.66	4350	7801	0.0016	92.97%	86.91%
Fruit fly	13.0039	0.4956	0.3616	235	279.39	303.31	0.2	99.43%	99.43%
Coral	142.62	0.1070	0.2565	376.49	376.871	157.20	0.0016	91.43%	88.99%

ρ_{LLPM} stands for CCC value linking to the LLPM of Equation (9), ρ_{LOG} denotes CCC produced by a fit of the logistic model of Equation (19).

We first considered data on yeast growing under ideal conditions in a test tube portrayed in Figure 45.10a) in Avisar et al. (2013) and reproduced here in Figure 4a. We know that the yeast growth curve shown in Panel (a), as portrayed in Avisar et al. (2013), suggests an inconsistent placement of the initial condition x_0 . Nevertheless, blue lines in Figure 4b display a consistent S-shaped curve fitted by the logistic model of Equation (19) on yeast data ($a = 0.2056, x_0 = 0.2998, K = 12.57, \rho = 98.19$). Afterwards, we produced a fit of Liebig's law of the minimum-driven model of Equation (9) (LLPM) to yeast data. Fitted LLPM parameters values were $a = 0.2549, b = 0.0452, x_0 = 1.1, R_0 = 8.1388$ and $p = 0.5$, which through Equations (10) and (11) produced $E = 5.7925$ and $K = 12.827$ one to one. Concurring reproducibility index value was $\rho = 99.23$. Comparing the shapes of the trajectories of the yeast population displayed in Figure 4, we can be aware that blue lines fitted by the present LLPM (Panel c) consistently describe an S-shaped pattern. Panel (c) also shows the shape of the fitted form of the resource abatement function $R(t)$ as given by Equation (3) (red lines). Avisar et al. (2013) do not refer to whatever energy source the yeast population depended on, but in any event, the shape of the fitted form of $R(t)$ suggests that independently of bulk consumption, the yeast population and its feeding resource stabilised one to one.

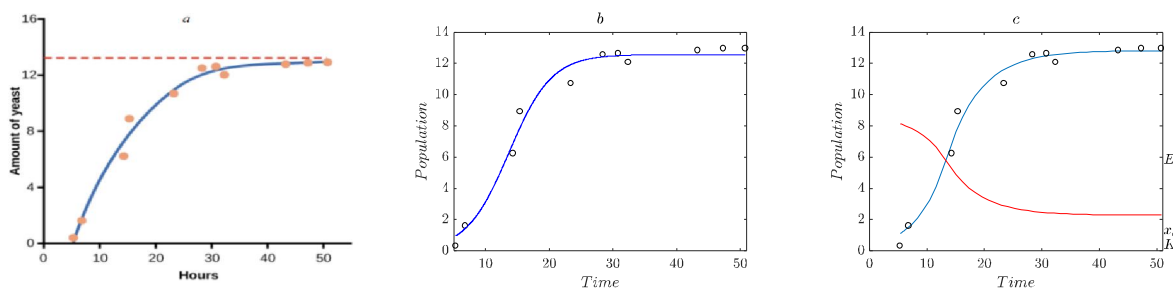


Figure 4: Yeast growth data from Avisar et al. (2013). Panel (a) is an assumed S-shaped logistic growth curve pattern associated with yeast grown under ideal conditions in a test tube, as in

Figure 45.10a in Avissar et al. (2013). Panel (b) displays a fit of the logistic model as given by Equation (19) to referred yeast data (blue lines). Panel (c) exhibits the spread of observed data points about the $x(t)$ trajectory resulting by fitting LLPM, Liebig's law of the minimum-driven model of Equation (9), to the yeast growth data adapted from Panel (a) (blue lines). Panel (c) also shows the shape of the fitted form of the resource abatement function $R(t)$ as given by Equation (3) (red lines).

Figure 5a presents the harbour seal population data in Figure 45.10b in Avissar et al. (2013). Figure 5b presents the spread of referred seal data about the logistic curve fitted by the model of Equation (19). Concordance Correlation Coefficient resulted in a value of $\rho = 86.91$, and parameter estimates were $a = 0.2986$, $K = 7459.08$, $x_0 = 1104.15$. Figure 5c shows the spread of captured seal data about the trajectory produced by a fit of LLPM, Liebig's law of the minimum-based model of Equation (9). Corresponding fitted parameters values were $a = 0.3142$, $b = 0.1748$, $x_0 = 1634.2444$, $R_0 = 4350$, and $p = 0.0016$, which employing equations (10) and (11) produced $E = 4345.6617$ and $K = 7801$ one to one. The reproducibility index acquired a value of $\rho = 92.97$. The associating form of $R(t)$ (red lines in Panel (c)) suggests that the steady form of the LLPM given by Equation (15) also fits consistently. This fact explains by the small fitted value for the parameter p . Moreover, Panel (d) displays a close-up look at the variation of $R(t)$, corroborating that this function remained close to its initial value independently of consumption by the seal population.

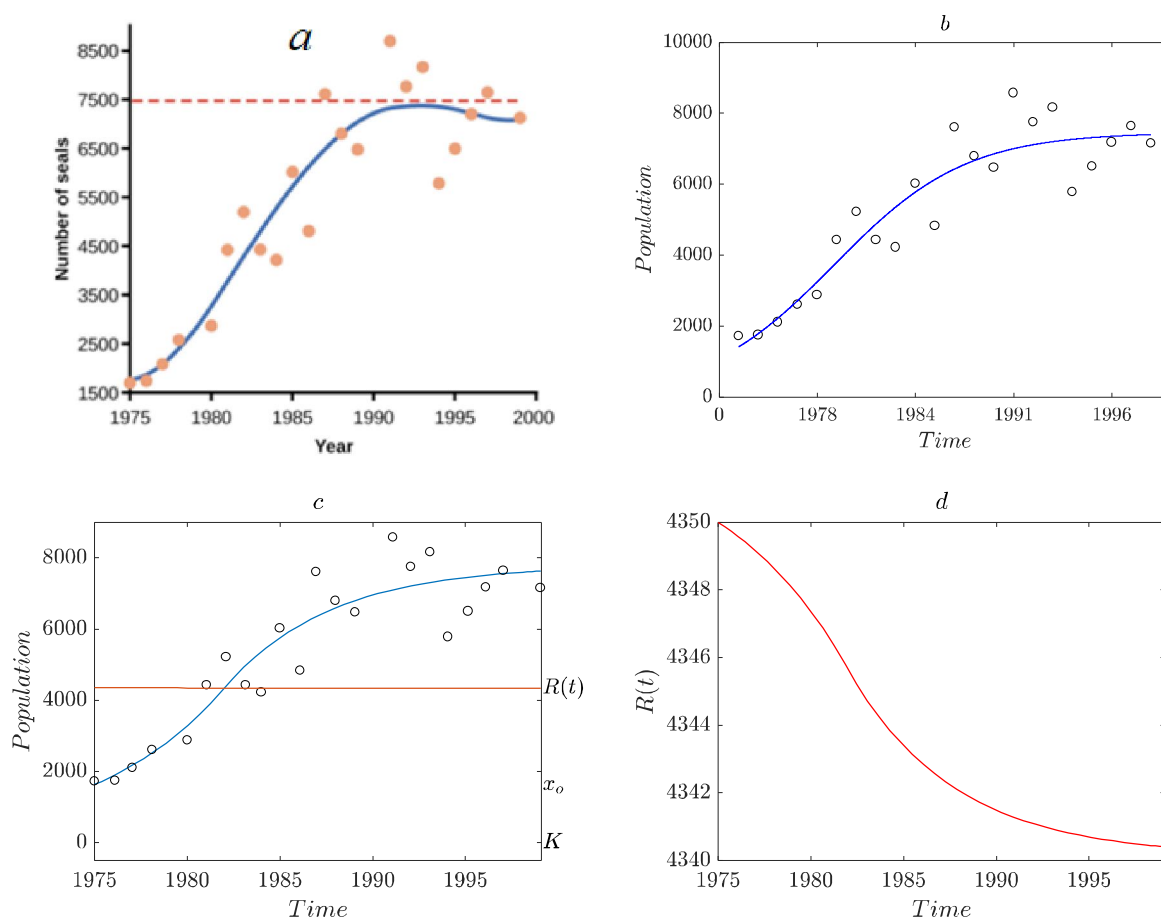


Figure 5: Fit of the LLPM on seal population growth data as reported in Avissar et al. (2013). Panel (a) is a presumed logistic growth curve pattern associated with a harbour seal population, as portrayed in Figure 45.10b in Avissar et al. (2013). Panel (b) exhibits the spread of the Avissar et al. (2013) harbour seal data about curves fitted by the conventional logistic model of Equation

(19). Panel (c) shows data spread about the $x(t)$ trajectory resulting by fitting LLPM Liebig's law of the minimum-driven model of Equation (9) to the available seal population growth data—panel (d) variation of the fitted resource availability function $R(t)$.

Correspondingly, Figure 6a presents the spread of data reported by R. Pearl on the growth of *Drosophila melanogaster* (Pearl, 1927) about the logistic curve fitted by the model of Equation (19). Fitted parameter values were $a = 6.19$, $K = 329.7$, $x_0 = 0.2194$ and with Concordance Correlation Coefficient at a value of $\rho = 99.43$. Figure 6b shows the spread of captured *Drosophila melanogaster* data about the trajectory produced by a fit of LLPM, Liebig's law of the minimum-based model of Equation (9). Fitted parameters values were $a = 0.4956$, $b = 0.3616$, $R_0 = 279.3992$, $x_0 = 13.0039$, $p = 0.2$, which through Equations (10) and (11) produced $E = 235$ and $K = 303.31$ one to one. Red lines on panel b display the variation of feeding resource availability $R(t)$, showing that although population consumption induced an asymptotical approach to a value K , resource abatement was moderate.

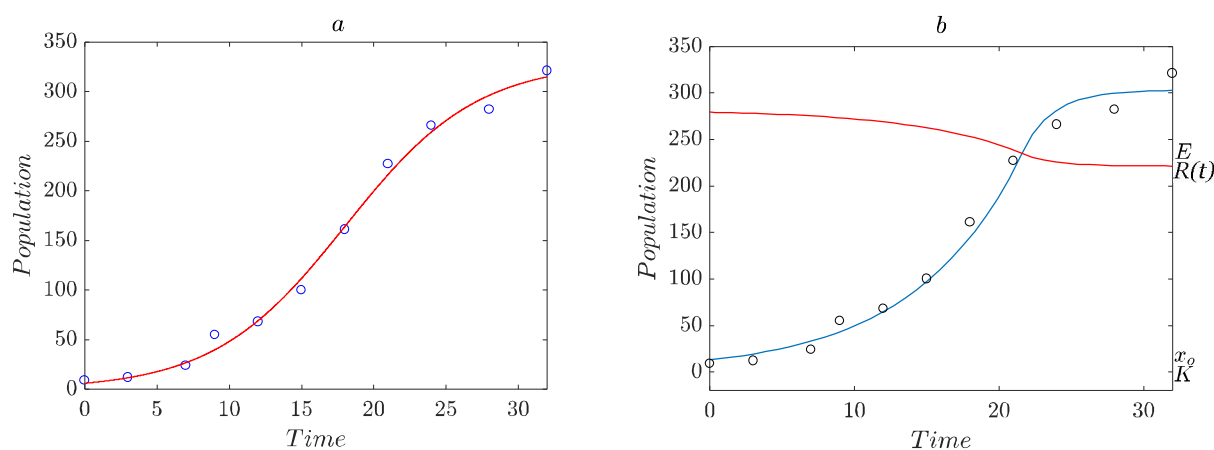


Figure 6: Fit of LLPM on *Drosophila melanogaster* growth data presented in Pearl (1927). Panel (a) displays a fit of the logistic model as given by Equation (19) to *Drosophila melanogaster* data, with Panel (b) exhibits the spread about the $x(t)$ trajectory resulting by fitting the Liebig's law of the minimum-driven model of Equation (9) to *Drosophila melanogaster* data. This last Panel also shows the shape of the fit of the resource abatement function $R(t)$ as given by Equation (3).

Finally, Figure 7a presents the spread of data reported by Hughes and Tanner (2000) on the decline of an *Agaricia agaricites* population on Jamaican reefs about the logistic curve fitted by the model of Equation (19) with $a = -0.1357$, $K = -1.7040$, $x_0 = 126.59$ and a Concordance Correlation Coefficient of $\rho = 88.99$. This fit identified the declining branch of the logistic model. However, it resulted in incompatibly negative values for the parameters a and K . Figure 7b shows the spread of captured *Agaricia agaricites* data about the trajectory produced by a fit of Liebig's law of the minimum-based model of Equation (9). Fitted parameters values were $a = 0.1070$, $b = 0.2565$, $R_0 = 376.871$, $x_0 = 142.6281$, $p = 0.0016$, which employing

Equations (10) and (11) produced $E = 376.49$ and $K = 157.20$, one to one. Compared to an unreliable fit of the logistic model shown in Panel b), an LLPM try predicts the extinction of the *Agaricia agaricites* population. In coherence, the LLPM predicts that the feeding resource path adapts to a steadily growing pace of stabilisation (panel c). Then regardless of plentiful feeding energy, the *Agaricia agaricites* population vanished away.

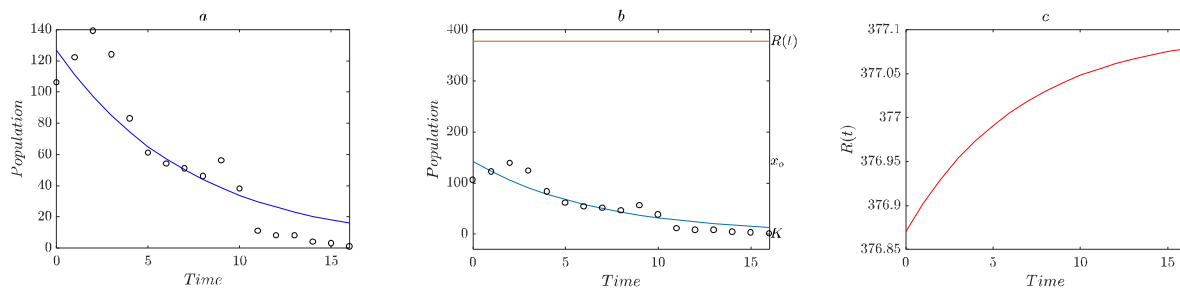


Figure 7: Fitting results of the LLPM on *Agaricia agaricites* growth data presented in Hughes and Tanner (2000). Panel (a) displays a fit of the logistic model given by Equation (19) to *Agaricia agaricites* data. Panel (b) exhibits the spread about the $x(t)$ trajectory resulting by fitting Liebig's law of the minimum-driven model of Equation (9) to *Agaricia agaricites* data and also shows the shape of fitted form of the resource abatement function $R(t)$ as given by Equation (3). Panel (c) close-up at the $R(t)$ variation.

IV. DISCUSSION

In cellular structures such as mitochondria, the maxima or minima of a periodical chemical reaction proved to be determinants of observable patterns (Woodcock, 1978). In other processes, for instance, catalysis, limiting values of variables such as pH and temperature can cause enzymes to lose their functionality, thereby impairing the easing of essential chemical reactions within living organisms (Dyson & Noltmann, 1968). Besides, the maximum and minimum blood glucose levels, body temperature, or pH range are critical for maintaining homeostasis (Yildiz et al., 2020). Furthermore, maximum and minimum values can activate regulatory mechanisms in biological systems that help organisms deal with and adapt to challenging environmental conditions. Within these response mechanisms, we can include activation of heat shock proteins that shield cells from harm given extreme values of temperature or water conservation mechanisms in plants in response to extreme osmotic conditions (Bich et al., 2016; Sharp et al., 1999; Chaves & Oliveira, 2004). Another example of extreme value control of a biological process is the existence of a minimum light intensity needed for efficient photosynthesis in plants (Boardman, 1977; Madsen & Sand-Jensen, 1994). What is more, in this vein, it is worth mentioning that extreme levels of light intensity or CO₂ concentrations can restrict the effectiveness of photosynthesis and, as a result, hamper the capability of plants to create energy (Jolliffe & Tregunna, 1968). Therefore, from a general perspective, comprehending the upper and lower limits of biologically relevant variables delivers an understanding of organisms' underlying limits, adaptive responses, and constraints.

In ecological settings, extreme values are often more descriptive of relevant dynamics than standard measures of central tendency (Gaines & Denny, 1993; Montiel et al., 2004). Issues relating to physical stress, such as high or low temperatures, salinity, soil water content, wind velocities, and varying durations of air exposure, serve as examples (Denny & Deines, 1990). Moreover, characterising extreme values not only aids in defining the optimal operational boundaries for ecological processes and contributes to our interpretation of the correlation between organisms and their environment (Ruthsatz, Dausmann, and Peck, 2022). For instance, species interaction dynamics and community formation depend on the maximum and minimum values of different variables (Checa et al., 2014). Furthermore, the availability of particular resources can limit the distribution of species or the sizes of their populations (Wright, 1983), while the sizes of predator populations below or above given edges can impact the distribution and behaviour of prey species (Schneider, 2001). Also, from an ecological perspective,

acknowledging the relevance of maximum and minimum values of pertinent variables contributed to conceiving the concept of tolerance bounds (Niinemets & Valladares, 2008; Pörtner, 2001; Goss & Bunting, 1976). For example, the minimum oxygen concentration required for aquatic organisms' survival sets their tolerance lower limit (Seibel, 2011; Gaufin et al., 1974). Likewise, the maximum temperature at which an organism can survive or reproduce entails its thermal tolerance upper limit (Madeira et al., 2012; Buckley & Huey, 2016). Ecological niches, characterised by certain variables' upper and lower limits, determine a species' optimal environmental conditions (Galparsoro et al., 2009). Therefore, including maximum and minimum thresholds for factors such as temperature, moisture, or nutrient availability helps to understand how organisms distribute and their ecological requirements (Kearney, 2006). Moreover, the notion of extreme value control significantly contributed to conceiving important theoretical constructs in ecological research, such as the Principle of Limiting Factors, developed based on results reported by Justus Von Liebig in 1843 (Liebig, 1843), the Law of Tolerance conceived by Victor Ernest Shelford in the early 20th century. Moreover, the Theory of the Niche, first proposed by the ecologist G. Evelyn Hutchinson in 1957, states that each species has a range of environmental conditions in which it can thrive (Hutchinson, 1957; Hutchinson, 1978; Polechová & Storch, 2008).

In summarising the passage above, it is worth emphasising that to understand better the underlying limits, changes, and necessities of living organisms; it is essential to determine the upper and lower limits that set the intervals of influence of their determining physical and biological variables. This understanding of suitable extreme values assists in setting the boundaries that biological processes must function within, leading to a better comprehension of how organisms work in conjunction with their surroundings to function efficiently. Notwithstanding, when referring to conceiving constructs aimed to model population dynamics, besides a reduced number of papers (e.g. Polyetayev, 1971; Echavarría & Gomez, 1979; Echavarría-Heras et al. 2021 Montiel-Arzate et al. 2004; Echavarría-Heras et al., 2021) the relevance of including extreme values of causal variables in a dynamical set up has not been adequately acknowledged in the literature. For that reason, we decided to further contribute to the matter, so, in this work, we modified the protocol by Echavarría-Heras et al. (2021) that resulted in the construct given by Equation (9), which we refer to as LLPM, for a single species population growth model, built upon Liebig's Principle of Limiting Factors. The LLPM sustains by hypothesising that: (1) the inherent natural natality rate is determined according to Liebig's Law by the minimum between the size of the population $x(t)$ and that of its feeding resource, $R(t)$, at a time t , (2) the accompanying natural mortality rate is supposed to be proportional solely to population size, and (3) the rate of consumption of the external feeding resource ostensibly varies directly proportional to the natural growth rate of the population. Despite being partially founded on the assumption that mortality depends linearly on population size, the qualitative exploration of the behaviour of the global trajectory associated with the offered LLPM demonstrated a proven capability to mimic the typical s-shaped pattern associated with restricted growth models. The presented fitting results confer the LLPM of excellent reproducibility features and reveal that such a paradigm offers a remarkable interpretative strength. Firstly, the LLPM could identify the suggested form for the resource abatement function $R(t)$ on the fly, entailing a feature that the typical logistic growth model of Equation (19) lacks. Secondly, also compared to the presently addressed logistic model, the LLPM offers a consistent way to identify a declining pace in population size leading to extinction which the latter model could not suitably achieve. Besides, simplifying complexity has been proven advantageous in finding parameter estimates for consistent reproducibility of real data sets.

Nevertheless, performing research on further simplifying the nonlinear parameter estimation tasks seems necessary.

V. APPENDIX. ANALYTICAL APPROACH

5.1 Continuity property of the global trajectory $x(t)$

Equation (12) states that the global trajectory $x(t)$, associating to the piecewise-defined ODE given by Equation (9), expresses such that

$$x(t) = \begin{cases} x_1(t) = x_{10}e^{(a-b)t} & \text{for } x(t) \leq E \\ x_2(t) = x_{20}e^{-(ap+b)t} + K(1 - e^{-(ap+b)t}) & \text{for } x(t) > E \end{cases} \quad (A1)$$

where agreeing to Equations (10) and (11), we have

$$E = (R_0 + px_0)/(1 + p)$$

and

$$K = aE(p + 1)(ap + b)^{-1}$$

with p , as explained around Equation (3), stands for the constant of proportionality between the resource consumption and natural population growth rates.

The constants x_{10} and x_{20} values in Equation (A1) follow from the requirement that $x(0) = x_0$ along with the continuity condition $x_1(t_c) = x_2(t_c)$, being t_c a time value such that $x(t_c) = E$. The value of t_c is determined depending on the ordering relationships between a and b , along with the placement of the initial condition $x(0) = x_0$ relative to the E threshold. Two ordering arrangements prompt the global $x(t)$ trajectory to cross the E threshold. The first one involves $a > b$ and $x_0 \leq E$, and another composing $a < b$ and $x_0 > E$.

5.2 Continuity of the global trajectory $x(t)$ in the case $a > b$ and $x_0 \leq E$

Assume that we have $a > b$ and $x_0 \leq E$. Then, at the beginning of the growth process, the global trajectory $x(t)$ shapes according to the $x_1(t)$ branch holding in the domain $x(t) \leq E$ and given by Equation (A1). Then to accomplish the suitable form $x_1(t)$, we must choose $x_{10} = x_0$; that is, we acquire

$$x_1(t) = x_0 \exp((a - b)t) \quad (A2)$$

According to Equation (A1), the complementary branch $x_2(t)$ of the global trajectory $x(t)$, holding in the domain $x(t) > E$, depends on the initial condition x_{20} , whose value ought to be determined. For that aim, we must enforce that the global trajectory $x(t)$ is continuous at a time $t = t_c$ such that $x(t_c) = E$ or equivalently $x_1(t_c) = E$ and $x_2(t_c) = E$. Therefore, we first need to obtain t_c . For achieving that task, we rely on the statement $x_1(t_c) = E$, so, using Equation (A2), we must have

$$x_0 e^{(a-b)t_c} = E,$$

from which solving for t_c yields

$$t_c = \ln (E/x_0)/(a - b) \tag{A3}$$

Secondly, we need to consider that continuity of $x(t)$ at $t = t_c$ fulfils if and only if $x_2(t)$ also satisfies $x_2(t_c) = E$. Agreeing with Equation (A1), this statement requires adapting a suitable value of the initial condition x_{20} , which makes

$$x_{20} e^{-(ap+b)t_c} + K(1 - e^{-(ap+b)t_c}) = E \tag{A4}$$

Then, solving for x_{20} , we obtain

$$x_{20} = (E - K)e^{(ap+b)t_c} + K$$

Moreover, equivalently replacing t_c , as given by Equation (A3), one gets

$$x_{20} = (E - K) \left(\frac{E}{x_0} \right)^{\frac{ap+b}{a-b}} + K. \tag{A5}$$

Being x_{20} identified, we can obtain the form of the $x_2(t)$ branch joining the initial one $x_1(t)$ to compose the global trajectory $x(t)$.

5.3 Continuity of global trajectory $x(t)$ in the case $a < b$ and $x_0 > E$

In turn, for $a < b$ and $x_0 > E$, agreeing to Equation (A1), the first portion of the global trajectory $x(t)$, turns out to be

$$x_2(t) = x_0 e^{-(ap+b)t} + K(1 - e^{-(ap+b)t}) \tag{A6}$$

Then, to complete the path $x(t)$, we need to get the complementary portion $x_1(t)$ holding in the domain $x(t) \leq E$. As stated by Equation (A1) requires adapting the value of the associating initial condition x_{10} such that the property that $x(t)$ is continuous at a time $t = t_c$ for which $x_2(t_c) = E$ succeeds. Again, this entails both $x_2(t_c)$ and $x_1(t_c)$ taking a common value E . From Equation (A6), the statement $x_2(t_c) = E$ leads to

$$x_0 e^{-(ap+b)t_c} + K(1 - e^{-(ap+b)t_c}) = E,$$

which in turn, allows solving for t_c namely

$$t_c = \ln (x_0 - K/E - K)(ap + b)^{-1} \tag{A7}$$

Correspondingly, using Equation (A1) to express the condition $x_1(t_c) = E$, then solving for x_{10} yields

$$x_{10} = E \exp(-(a - b)t_c),$$

from which, after replacing t_c as given by (A7), leads to

$$x_{10} = E \left(\frac{x_0 - K}{E - K} \right)^{-\frac{a-b}{ap+b}} \tag{A8}$$

5.4 Construction of the global trajectory $x(t)$ for the case $a < b$

Whenever $a - b < 0$ and $x_0 \leq E$, initially the $x(t)$ dynamics sets by $x_1(t)$ as given by Equation (A2) namely

$$x_1(t) = x_0 \exp(a - b) t.$$

Then, $x_1(t)$ is decreasing for all $t \geq 0$. Therefore, $x(t) \leq x_0 < E$ for $t \geq 0$. Consequently, the global trajectory $x(t)$ maintains the $x_1(t)$ shape for $t \geq 0$. Besides, we have

$$\lim_{t \rightarrow \infty} x_1(t) = 0. \tag{A9}$$

Because of this, the population size $x(t)$ vanishes according to an exponential law.

Assume now that $a < b$ and $x_0 > E$. Then, initially, $x(t)$ will conform to $x_2(t)$ as given by Equation (A6), that is,

$$x_2(t) = x_0 e^{-(ap+b)t} + K(1 - e^{-(ap+b)t})$$

Since by assumption $a < b$ and we also have $E > 0$, it follows that,

$$aE(p + 1) < (pa + b)E \tag{A10}$$

Since as it is stated by Equation (A1), we have $K = aE(p + 1)(ap + b)^{-1}$, inequality (A10) along the statement, $x_0 > E$ yield the ordering,

$$K < E < x_0 \tag{A11}$$

On the other hand, from Equation (A6), the derivative of $x_2(t)$ becomes.

$$dx_2(t)/dt = (ap + b)(K - x_0)e^{-(ap+b)t} \tag{A12}$$

Since $(ap + b)e^{-(ap+b)t} > 0$ for $t \in \mathbb{R}^+$, the sign of $\frac{dx_2(t)}{dt}$ shall be fixed by the factor $(K - x_0)$.

Then, since inequality (A11) holds, we have $x_0 > K$, which implies $\frac{dx_2(t)}{dt} < 0$. Hence, for $a < b$ and $x_0 > E$, we have established that $x(t)$ becomes a decreasing function of time t . On the other hand, from Equation (A6), we also have that

$$\lim_{t \rightarrow \infty} x_2(t) = K. \tag{A13}$$

Therefore, the $x_2(t)$ path bears a horizontal asymptote K . Note also that because $a < b$, by inequality (A11), we also have $K < E$. Therefore, the limiting value of $x_2(t)$ whenever $t \rightarrow \infty$ will lie below E . Then, necessarily the $x_2(t)$ trajectory keeps on decreasing until it reaches the value E , that is, there exists a time value $t = t_c$ as given by Equation (A7) such that $x_2(t_c) = E$ and after that, the dynamics of $x(t)$ will set by $x_1(t)$, that according to Equation (A1) bears a form

$$x_1(t) = x_{10} \exp(a - b) t.$$

Then, choosing

$$x_{10} = E \exp(-(a - b)t_c),$$

adds the continuity condition $x_1(t_c) = E$, as much as setting $x(t)$ to decrease asymptotically towards zero (see Figure A1b).

We can summarise what we have explored so far by stating that maintenance of the condition $a < b$ implies the disappearance of the population, regardless of its initial value x_0 (also regardless of whether this value is greater or equal or less than E).

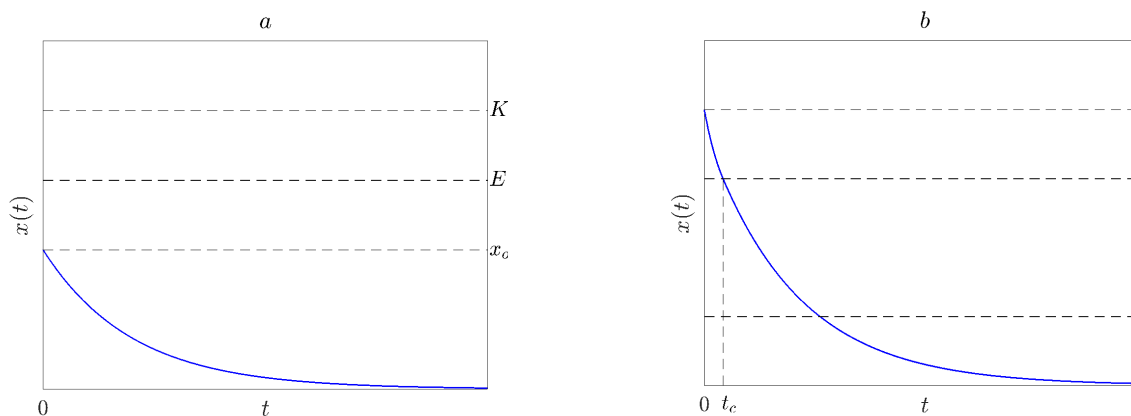


Figure A1: Construction of the $x(t)$ trajectory for $a < b$. Provided $a < b$, then for $x_0 \leq E$, the population size $x(t)$ vanishes following the exponential law $x_1(t)$ given by Equation (A1) with $x_{10} = x_0$ (Panel a). For $a < b$ and $x_0 > E$, initially $x(t)$ takes on an $x_2(t)$ form given by Equation (A1), which decreases asymptotically to a value $K < E$. When crossing the horizontal line $x = E$, at a time t_c , the trajectory $x(t)$ ceases to be given by $x_2(t)$ that would take it to the limit value K by t approaching infinity and begins following an $x_1(t)$ shaped trajectory with $x_{10} = E e^{-(a-b)t_c}$. Therefore, $x(t)$ will asymptotically progress to zero as t approaches infinity.

5.5 Construction of the $x(t)$ trajectory for the case $a > b$

Now suppose that inequality $a > b$ fulfils. Then, $E > 0$ implies

$$aE(p + 1) > (pa + b)E.$$

Now, since Equation (A1) establishes, $\frac{K=aE(p+1)}{(ap+b)}$, inequality above implies the ordering

$$K > E \tag{A14}$$

Suppose that $a - b > 0$ and $x_0 \leq E$. Under these conditions, as specified by inequality (A14), we also have the $K > E$ order. And, as given by Equation (A2), at the beginning of the process, the population size $x(t)$ will be set by

$$x_1(t) = x_0 e^{(a-b)t}.$$

Then, once it departs from x_0 , $x_1(t)$ will increase exponentially. And, since $x_0 \leq E$, as we elaborated around Equation (A3) by continuity of the global trajectory $x(t)$, there will be a time $t = t_c$ satisfying,

$$t_c = \ln(E/x_0)/(a - b),$$

at which population size $x(t)$, as given by $x_1(t)$, will meet the E threshold, that is, $x_1(t_c) = E$. For $t > t_c$, according to Equation (A1), population size $x(t)$ will switch from the growth form $x_1(t)$ to the $x_2(t)$ one. Again, Equation (A12) states that the sign of $\frac{dx_2(t)}{dt}$ sets by the factor $(K - x_0)$. Then, $x_2(t)$ will increase whenever $E < x_0 < K$, and as stated by Equation (A13), $x_2(t)$ approaches K as t progresses to infinity (Figure A2a).

Assume that in addition to $a > b$, the initial condition x_0 places such that $E < x_0 < K$. Under these circumstances, the process will be conducted for a certain initial period by the $x_2(t)$ branch of the trajectory $x(t)$, as established by Equation (A6). Again, Equation (A12) states that the sign of $\frac{dx_2(t)}{dt}$ shall fix by the factor $(K - x_0)$. Then, $x_2(t)$ will increase whenever $E < x_0 < K$, and as stated by Equation (A13), $x_2(t)$ approaches K as t progresses to infinity (Figure A2a). Besides, whenever $a > b$ and $x_0 > K > E$, the population size $x(t)$ will be described by $x_2(t)$, attaining a form given by Equation (6), that is,

$$x_2(t) = x_0 e^{-(ap+b)t} + K(1 - e^{-(ap+b)t}).$$

Then, as we have elaborated above, the condition $x_0 > K$ sets the $x_2(t)$ branch of the global $x(t)$ trajectory to be decreasing and asymptotically approaching K as t progresses to infinity (Figure A2b).

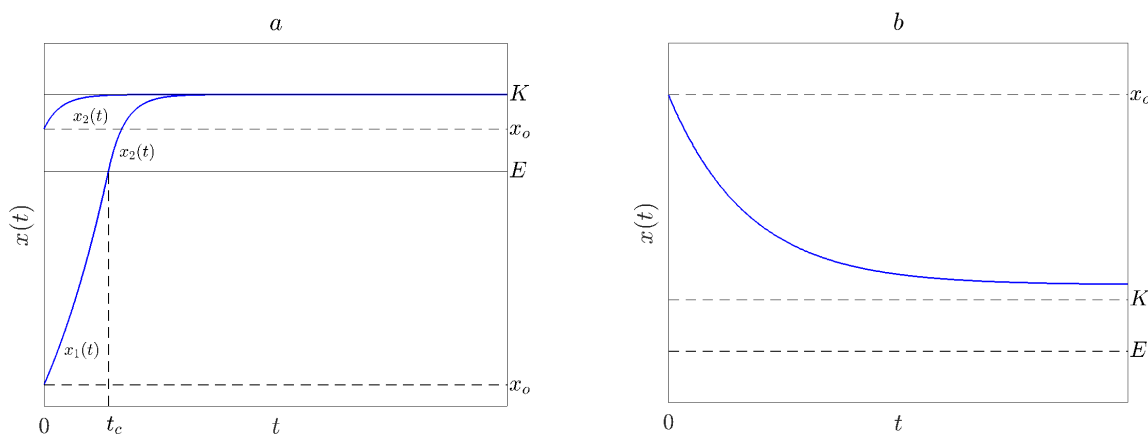


Figure A2: Construction of the $x(t)$ trajectory for $a > b$. Whenever $a > b$ and $x_0 \leq E$ at the beginning of the process, population size $x(t)$ will be ruled by $x_1(t)$ as given by Equation (9), and consequently, it will increase. By continuity, $x_1(t)$ will eventually reach the E threshold, and the dynamics will start to be modelled by the $x_2(t)$ branch of the global trajectory $x(t)$, thereby approaching the equilibrium level K when t progresses to infinity. The case $a > b$ and $E < x_0 < K$ portrays similarly with $x(t)$ behaving as the $x_2(t)$ branch and asymptotically approaching K (Panel a). Besides, whenever $a > b$ and $x_0 > K > E$, the population size $x(t)$ will be described by $x_2(t)$, so the condition $x_0 > K$ will fix $x(t)$ to be decreasing and asymptotically approaching K as t progresses to infinity (Panel b).

Summarising, whenever $a > b$, then either the, $0 < x_0 < E < K$ or $E < x_0 < K$ placements of the initial condition x_0 will drive the population size $x(t)$ being monotonically increasing and approaching K . If instead $x_0 > K$, $x(t)$ will be monotonically decreasing with K as an asymptote. As a consequence of this, $x(t) = K$ could stand as a specific equilibrium state of the system determined by a and b , the internal development processes that set the intensities of the natality and mortality processes ($N(t)$ and $M(t)$), as well as, by the external factor E .

5.6 Analysis of case $a = b$

Let us now analyse the behaviour of $x(t)$ for the case $a = b$. Again comparing x_0 and E , we may first consider the $x_0 \leq E$ order. As we already know, for this case, the behaviour of the trajectory $x(t)$ is determined by the $x_1(t)$ branch as given by Equation (A2), namely $x_1(t) = x_0 e^{(a-b)t}$. Then, since by assumption $a = b$, we have $x_1(t) = x_0$. The trajectory $x(t)$ remains stationary (Figure A3a).

For $a = b$ and $x_0 > E$, the $x(t)$ trajectory follows the $x_2(t)$ rule at the start of the growing process. According to Equation (A6) for $a = b$, becomes,

$$x_2(t) = x_0 e^{-a(p+1)t} + E(1 - e^{-a(p+1)t}) \tag{A15}$$

Then we have

$$\lim_{t \rightarrow \infty} x_2(t) = E \tag{A16}$$

Equation (A15) yields

$$dx_2(t)/dt = a(p + 1)(E - x_0)e^{-a(p+1)t} \tag{A17}$$

Nevertheless, since we established the condition $x_0 > E$, then $\frac{dx_2(t)}{dt} < 0$ so the $x(t)$ trajectory shall be decreasing and asymptotically approaching E as t progresses to infinity (Figure A3b).

In short, the case $a = b$ entitles a heterogeneous behaviour because if the magnitude of the initial population satisfies $x_0 < E$, then population size $x(t)$ remains steady. However, if the initial population size lies above the E threshold, i.e. $x_0 > E$, then $x(t)$ decreases exponentially and asymptotically approaches the equilibrium level E .

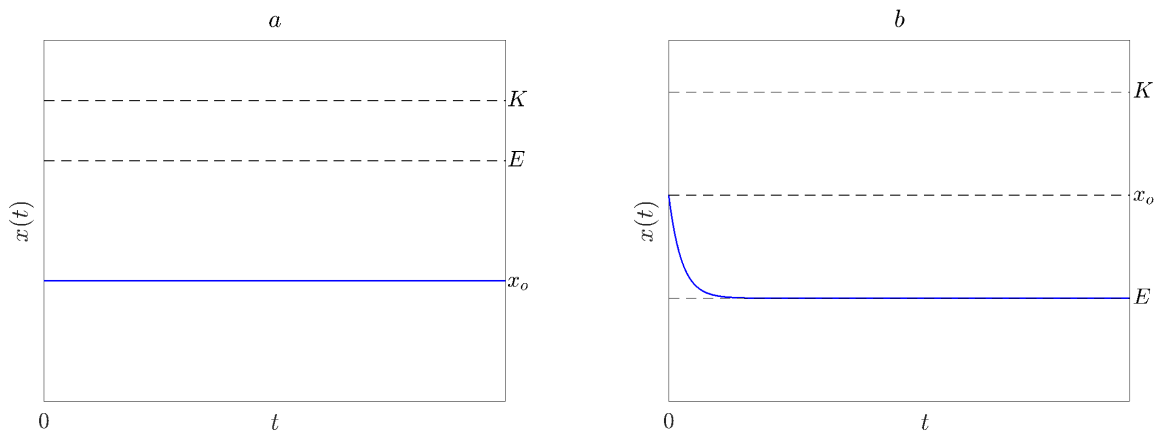


Figure A3: The shape of $x(t)$ for $a = b$. For $a = b$ and $x_0 \leq E$, the $x(t)$ trajectory remains stationary (Panel a). If the initial population size lies above the E threshold, i.e. $x_0 > E$, then $x(t)$ decreases exponentially and asymptotically approaches E .

Summarising, the case $a = b$ entitles a heterogeneous behaviour because if the magnitude of the initial population satisfies $x_0 < E$, then population size $x(t)$ remains steady. However, if the initial population size lies above the E threshold, i.e. $x_0 > E$, then $x(t)$ decreases and asymptotically approaches the E threshold.

ACKNOWLEDGEMENTS

The authors would like first to thank CICESE, our honourable and generous institution that this year celebrates its 50th anniversary and whose unrestricted support has allowed our Consolidation as scientists. Hector Echavarria Heras expresses special thanks to Guillermo Gómez Alcaraz for suggesting pursuing this research. We also thank three anonymous reviewers for their valuable and enlightening comments.

REFERENCES

1. Avissar Yael, Choi Jung, DeSaix Jean, Jurukovski Vladimir, Wise Robert, Rye Connie. (2013). Environmental Limits to Population Growth, In Biology, published by The OpenStax College, Rice University 1515 pp.
2. Anees S. (2022). The principle of space-for-time substitution in predicting betula spp. Biomass change related to climate shifts. *Applied ecology and environmental research*, 20(4), 3683–3698.
3. Bich L., Mossio M., Ruiz-Mirazo K. et al (2016). Biological regulation: controlling the system from within. *Biol Philos*, 31, 237–265.
4. Boardman N. T. (1977). Comparative photosynthesis of sun and shade plants. *Annual review of plant physiology*, 28(1), 355–377.
5. Buckley L. B. & Huey R. B. (2016). How extreme temperatures impact organisms and the evolution of their thermal tolerance. *Integrative and comparative biology*, 56(1), 98–109.
6. Charlebois D. A. and Balázsi G. (2018). Modeling cell population dynamics. *In Silico Biology*, 13(1-2), 21-39.
7. Chaves M. M. and Oliveira M. M. (2004). Mechanisms underlying plant resilience to water deficits: prospects for water-saving agriculture. *Journal of experimental botany*, 55(407), 2365-2384.
8. Checa M. F., Rodriguez J., Willmott K. R., & Liger B. (2014). Microclimate variability significantly affects the composition, abundance, and phenology of butterfly communities in a highly threatened neotropical dry forest. *Florida Entomologist*, 97 (1), 1–13.
9. Dyson J. E. D. and Noltmann E. A. (1968). The effect of pH and temperature on the kinetic parameters of phosphoglucose isomerase: Participation of histidine and lysine in a proposed dual function mechanism. *Journal of Biological Chemistry*, 243 (7), 1401-1414.
10. Denny, M. W. and Deines S. O. (1990). On the prediction of maximal intertidal wave forces. *Limnology and Oceanography*, 35 (1), 1-15.
11. Echavarría-Heras H. A., Leal-Ramírez C., Gómez G. and Montiel-Arzate E. (2021). Principle of Limiting Factors-Driven Piecewise Population Growth Model I: Qualitative Exploration and Study Cases on Continuous-Time Dynamics. *Complexity*, 2021, 1-24.
12. Echavarría, H. A. and Gómez A. G. (1979). El principio de los factores limitantes y el crecimiento de poblaciones. Comunicaciones Internas, Departamento de Matemáticas, Facultad de Ciencias UNAM, 13 (1979).
13. El-Sharkawy M. A. (2011). Overview: Early history of crop growth and photosynthesis modeling. *BioSystems*, 103 (2), 205-211.
14. Galparsoro, I., Borja, Á., Bald, J., Liria, P., & Chust, G. (2009). Predicting suitable habitat for the European lobster (*Homarus gammarus*) on the Basque continental shelf (Bay of Biscay), using Ecological-Niche Factor Analysis. *Ecological Modelling*, 220(4), 556-567.
15. Gaines S. O. & Denny M. W. (1993). The largest, smallest, highest, lowest, longest and shortest: Extremes in ecology. *Ecology*, 74 (6), 1677–1692.
16. Gaufin A. R., Clubb R. and Newell R. (1974). Studies on the tolerance of aquatic insects to low oxygen concentrations. *The Great Basin Naturalist*, 45-59.
17. Ghaleb A. A. S., Kutty S. R. M., Ho Y. C., Jagaba A. H., Noor A., Al-Sabaei A. M. and Almahbashi N. M. Y. (2020). Response surface methodology to optimise methane production from mesophilic anaerobic co-digestion of oily-biological sludge and sugarcane bagasse. *Sustainability*, 12 (5), 2116.
18. Goss L. B. & Bunting D. L. (1976). Thermal tolerance of zooplankton. *Water Research*, 10 (5), 387–398.
19. Hughes T.P. and Tanner J.E. (2000). Recruitment failure, life histories and long-term decline of Caribbean corals. *Ecology*, 81(8), 2250–2263.

20. Hutchinson G.E. (1957). Concluding remarks. *Cold Spring Harbor Symp* 22, 415–427.
21. Hutchinson G.E. (1978). *An Introduction to Population Ecology*. Yale Univ Press, New Haven, CT.
22. Jolliffe P. A. and Tregunna E. B. (1968). Effect of temperature, CO₂ concentration, and light intensity on oxygen inhibition of photosynthesis in wheat leaves. *Plant physiology*, 43(6), 902-906.
23. Kearney M. (2006). Habitat, environment, and niche: what are we modelling? *Oikos*, 115(1), 186-191.
24. Liebig V. J. F. (1843). *Chemistry in its application to agriculture and physiology*. (As quoted by E WRussell in *Soil Conditions and Plant Growth*), 10th Edn. London: Longman
25. Lin L.I.K. (1989). A concordance correlation coefficient to evaluate reproducibility. *Biometrics*, pp. 45, 255–268.
26. Madeira D., Narciso L., Cabral H. N. and Vinagre C. (2012). Thermal tolerance and potential impacts of climate change on coastal and estuarine organisms. *Journal of Sea Research*, 70, 32-41.
27. Madsen T. V. and Sand-Jensen K. (1994). The interactive effects of light and inorganic carbon on aquatic plant growth. *Plant, Cell & Environment*, 17 (8), 955-962.
28. Montiel-Arzate E., Echavarría-Heras H. and Leal-Ramírez C. (2004). A functionally diverse Population growth model. *Mathematical biosciences*, 187(1), 21-51.
29. Niinemets Ü. And Valladares F. (2008). *Encyclopedia of Ecology* Editor(s): Sven Erik Jørgensen, Brian D. Fath, Academic Press, 1370–1376.
30. Odum E. P. (1963). *Ecology*. Holt, Rine Hart and Winston, Inc.
31. Odum E. P. (1971). *Fundamentals of Ecology*, Third Edition, W. B. Saunders Co.
32. Pearl R. (1927). The growth of populations. *The Quarterly Review of Biology*, pp. 2, 532–548.
33. Peeters E. T. and Gardeniers A. J. J. (1998). Logistic regression as a tool for defining habitat requirements of two common gammarids. *Freshwater Biology*, 39(4), 605-615.
34. Polechová J. and Storch D. (2008). Ecological niche. *Encyclopedia of ecology*, 2, 1088-1097.
35. Polyetayev I. A. (1971). Modeli Volterra, Jishnir-Zhertva y Nekotorye ij obobschenyas. Ispolzovainien Printsipa Liebija, *Zhurnal Obshei Biologii*, 34(1), 43-57.
36. Pörtner H. (2001). Climate change and temperature-dependent biogeography: oxygen limitation of thermal tolerance in animals. *Naturwissenschaften*, 88, 137-146.
37. Rizhinashvili, A. L. (2022). An Outline of the Theory of the Functioning of Aquatic Ecosystems: Nutrient Limitation. *Biology Bulletin Reviews*, 12(6), 596–608.
38. Ruthsatz K., Dausmann, K. H. Peck M. A. and Glos J. (2022). Thermal tolerance and acclimation capacity in the European common frog (*Rana temporaria*) change throughout ontogeny. *Journal of Experimental Zoology Part A: Ecological and Integrative Physiology*, 337(5), 477-490.
39. Seibel B. A. (2011). Critical oxygen levels and metabolic suppression in oceanic oxygen minimum zones. *Journal of Experimental Biology*, 214(2), 326–336.
40. Schneider M. F. (2001). Habitat loss, fragmentation, and predator impact: spatial implications for prey conservation. *Journal of Applied Ecology*, 38(4), 720-735.
41. Sharp F. R., Massa S. M. and Swanson R. A. (1999). Heat-shock protein protection. *Trends in neurosciences*, 22 (3), 97-99.
42. Shelford V. E. (1913). *Animal Communities in Temperate North America*, Univ. Chicago Press.
43. Sprengel K. (1839). *Die Lehre vom Dünger oder Beschreibung aller bei der Land wirth schaft gebräuchlicher vegetabilis cher, animalischer und mineralischer Dünger Materialien, nebst Erklärung ihrer Wirkung Art*. Leipzig.

44. Verhulst P. F. (1838). Notice sur la loi que la population suit dans son accroissement. *Correspondence mathématique et physique*, 10, 113-129.
45. Wright D. H. (1983). Species-energy theory: an extension of species-area theory. *Oikos*, pp. 496–506.
46. Woodcock A. E. R. & Davis M. (1978). *Catastrophe Theory*, E. P. Dutton, New York.
47. Yildiz C., Bilgin V. A., Yilmaz B. and Özilgen M. (2020). Organisms live at far-from-equilibrium with their surroundings while maintaining homeostasis, importing exergy, and exporting entropy. *International Journal of Exergy*, 31(3), 287-301.

This page is intentionally left blank



Scan to know paper details and
author's profile

Structural and Dielectric Studies of Ni doped TiO₂ Thin Films for Electro-Optic Devices

Davinder Singh, Rajesh Kumar, K. K. Saini & Nafa Singh

Kurukshetra University

ABSTRACT

Pure and Ni doped TiO₂ thin films are prepared by sol-gel dip coating technique and sintered at 500 °C. Particle size decreases from 40 nm to 20 nm in case of 10 mol% Ni doped TiO₂ thin films. XPS studies reveal that titanium exists in Ti⁺⁴ state in pure and Ni doped TiO₂ thin films. MOS structures are formed by fabricating the ITO bottom electrode and Al top electrode. The thickness of all the Ni doped TiO₂ thin films is nearly 140 nm as measured by thickness profilometer. Dielectric constant and dielectric loss decreases with increase in frequency. Anatase phase has been found in pure and Ni doped TiO₂ thin films. Density of interfacial states measured with the help of measured values of capacitances.

Keywords: TiO₂, sintering temperature, anatase, dielectric constant, density of interfacial states.

Classification: LCC: TK

Language: English



Great Britain
Journals Press

LJP Copyright ID: 925692

Print ISSN: 2631-8490

Online ISSN: 2631-8504

London Journal of Research in Science: Natural and Formal

Volume 23 | Issue 9 | Compilation 1.0



Structural and Dielectric Studies of Ni doped TiO₂ Thin Films for Electro-Optic Devices

Davinder Singh^α, Rajesh Kumar^σ, K. K. Saini^ρ & Nafa Singh^ω

ABSTRACT

Pure and Ni doped TiO₂ thin films are prepared by sol-gel dip coating technique and sintered at 500 °C. Particle size decreases from 40 nm to 20 nm in case of 10 mol% Ni doped TiO₂ thin films. XPS studies reveal that titanium exists in Ti⁺⁴ state in pure and Ni doped TiO₂ thin films. MOS structures are formed by fabricating the ITO bottom electrode and Al top electrode. The thickness of all the Ni doped TiO₂ thin films is nearly 140 nm as measured by thickness profilometer. Dielectric constant and dielectric loss decreases with increase in frequency. Anatase phase has been found in pure and Ni doped TiO₂ thin films. Density of interfacial states measured with the help of measured values of capacitances.

Keywords: TiO₂, sintering temperature, anatase, dielectric constant, density of interfacial states.

Corresponding Author α: Davinder Singh having M.Sc in Physics from M.D. University Rohtak in 1998 and Ph.D Physics from Kurukshetra University, Kurukshetra in 2012. Govt. College Faridabad, Haryana (India).

ρ: National Physical Laboratory, New Delhi (India).

ω: Kurukshetra University, Kurukshetra, (India).

I. INTRODUCTION

In the few recent years experimental investigation on the electronic transport properties of semiconducting oxides in thin films have been much intensified. Titanium oxide thin films have attracted much attention because of their applications in microelectronics devices, optical thin film devices, gas sensors etc. The structural and semiconducting properties of TiO₂ films can be strongly modified by doping with impurities like In, Cr, Cd, Ce, and Fe or by different processing parameters [1].

Evaluation of electrical properties is important in understanding the conduction mechanism. Critical evaluation of these properties is necessary to produce reproducibly good quality films. Electrical properties of transparent conducting TiO₂ thin films derived from methods other than sol-gel, have been investigated extensively and literature survey indicates a lot of scatter in experimental data due to variations in mobility and carrier concentration, arising as a consequence of variations in stoichiometry and dopant concentration (both intentional and unintentional). These two quantities are strongly dependent on the choice of processing method and the processing conditions. The development of methods for modification of dielectric and electrical properties of thin films of oxides is of great interest. Further studies have shown that ions of different transition and noble metals incorporated into titanium oxide as matrix could modify its optical and electrical properties [2]. The dielectric constant reported for TiO₂ thin films are scattered over a large range dependent on deposition methods, film thickness and process parameters. Various methods or techniques such as

electro deposition technique [3], Molecular chemical vapor deposition [4], Magnetron sputtering [5], Chemical spray pyrolysis [6], Sol-gel spin coating [7] technique are used to prepare these thin films. Each technique has its own advantages. We have used sol gel dip coating technique to prepare samples as this technique is cheaper and better uniformity is obtained by this technique.

Various authors study on the metal doped TiO₂ thin films, Cu doped TiO₂ thin films [8], Al doped TiO₂ thin films [9], Mn doped TiO₂ thin films, [10]. These pure and metal doped TiO₂ thin films have different types of applications i.e. in the manufacturing of LED [11], fabrication of capacitors in microelectronics [12], switching devices [13], integrated circuits (ICs) and field effect transistors (FETs) [14-15]. Modern technology demands scaling down the thickness of the material in order to increase the stability, performance and compact size of the electronic devices in accordance with the Moore law and quantum well effect [16]. Also the research work on dielectric response of TiO₂ doped by different percentage of Ta, and Ca or Nb, Ba has been carried out in literature [17-19]

Materials having dielectric constant in the range between 10-15 for frequencies above 1 GHz are practically utilized in treating biomedical modeling problems related to electromagnetic radiation scattering in the human organs such as liver, kidney, brain and tissues like fat and skin [20]. In this work we have investigated the dielectric properties of pure and Ni doped TiO₂ thin films, as doping modifies the electronic structure and dielectric properties of the material. Ni doped TiO₂ have shown several interesting properties like photocatalytic, hydrophilicity, optical and electrical properties. But the information and study about dielectric properties is limited.

II. EXPERIMENTAL

Partially hydrolyzed 0.5 molar solution of TiO₂ was prepared in isopropyl alcohol by adding equimolar ratios of titanium tetra butoxide and water. Nitric acid was used as a catalyst. Solution was refluxed for two hours and pure TiO₂ film was fabricated from this solution by sol-gel dip coating technique at a lifting speed of 24 mm/sec. To prepare Ni doped TiO₂ films a stock solution of the Ni acetylacetonate prepared in isopropyl alcohol. The calculated quantities of the stock solution were added to the undoped TiO₂ solution. The solution was stirred vigorously by magnetic stirrer using Teflon coated bit [21]. Identical processing parameters were maintained for all doped TiO₂ thin films. All the films were fabricated on ITO coated glass in vertical lifting geometry under tight control relative humidity and temperature maintained between 40-50% and 25-30 °C respectively. Dopant concentration was varied from 2 to 10 mol% for Ni doped TiO₂ thin films. Coated substrates were hanging in the vertical position for one minute to allow the excess solution at the bottom edge of the substrate to drip the solution. These samples were subsequently dried at the 100 °C for half an hour before sintering and then sintered at 500 °C for 1 hour.

To study dielectric properties Al/TiO₂ /ITO the heterostructure is prepared on the ITO coated glass. The top Al (aluminum) electrode is prepared by electron deposition technique and bottom ITO (indium tin oxide) electrode prepared by photolithography technique. The thickness of top Al electrode is 300 nm and the thickness of bottom ITO electrode is 500 nm as measured by thickness profilometer. Copper wires connected to top and bottom electrodes with the help of silver paste for dielectric measurements.

2.1 Characterization Techniques

X-ray photoelectron spectroscopy of the samples was conducted using Perkin Elmer 1257 with a hemispherical analyzer. The resolution of the instrument is 0.1 MeV. Accelerating voltage used for the analysis was 15 KV. It can detect all the elements except H and He. Dielectric measurements were

carried out in an electrically shielded plate condenser using HP 4192 A IMPEDANCE ANALYSER in the frequency range 20 Hz to 10 MHz. at room temperature.

III. RESULTS AND DISCUSSION

All the Ni doped TiO₂ films are highly stable and scotch resistant under investigations by scotch tape test and mechanically rubbing with cotton cloth using detergents. They were also found to be stable under harsh environments (containing vapors of different gases, acid fumes etc.) and under open environment (under sun) kept continuously for six months. Not even a single pin hole or scotch was developed in the films and they again passed scotch tape test after this treatment.

3.1 XRD studies

All the Ni doped TiO₂ films sintered at 500 °C for 1 hour exist in anatase phase as already reported [21] by Davinder et.al. The particle size goes on decreasing with increase in Ni content. The particle size decreased from 40 nm in case of 2 mol% Ni doped TiO₂ film to 20 nm in case of 10 mol % Ni doped TiO₂ thin film. The reason for this decrease in particle size is due to the introduction of Ni⁺² ions which change the surface charge of TiO₂ solution particles and the distances from each other. In this way The TiO₂ particles are most likely formed in the smaller size [22]. These results are in good agreement with the results reported in literature [23]

3.2 XPS Studies

XPS analysis of all the samples carried out on thin film samples coated on glass substrates by irradiating the samples with MgK α -X rays (1253.6 eV). Typical wide scan XPS spectra for the samples are shown in figure numbers 1(a), 1(b), 1 (c), 1(d), 1(e) and 1(f). In this study, the positions of binding energy corresponding to Ti 2p_{3/2} and Ti 2p_{1/2} lines for pure TiO₂ films were found at 457.95 eV and 463.6 eV; these indicate the presence of Ti⁴⁺ in TiO₂ film. The binding energies of Ti 2p for the Ni-doped samples were almost the same as those for pure TiO₂ film, except that the XPS peaks slightly broadened in doped films containing more than 4 mol% nickel oxide. Titanium also in the Ti⁴⁺ oxidation state in all the doped TiO₂ films. Oxygen in the films was in the form of O²⁻ in TiO₂ and NiO. The O 1s peak, which broadened to a higher binding energy position associated with the surface hydroxide, could be seen in films 2 mol% Ni doped TiO₂ and 6 mol% Ni doped TiO₂ with the small amounts of nickel. The redox potential for photo-generated holes is +2.53 V versus the standard hydrogen electrode (SHE) [24] after reaction with the hydroxide; these holes can produce hydroxyl radicals (\cdot OH) whose redox potential is only slightly decreased.

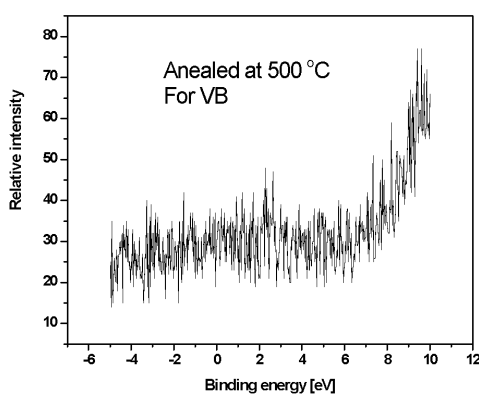


Fig. 1.(a)

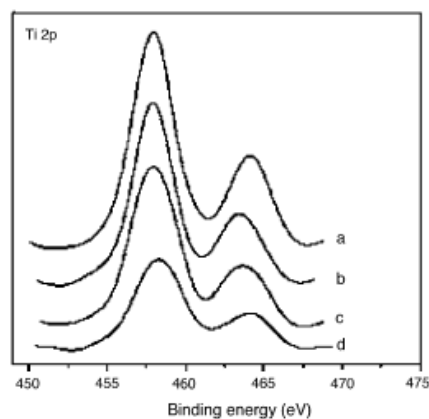


Fig. 1.(b)

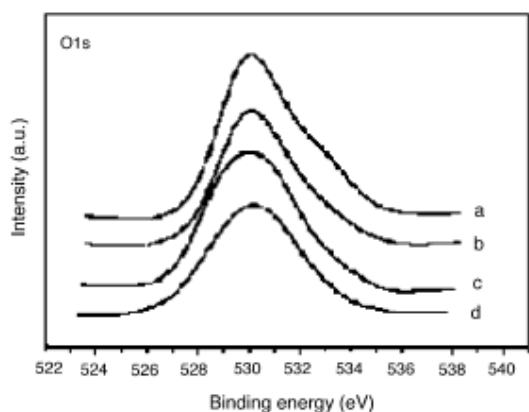


Fig. 1.(c)

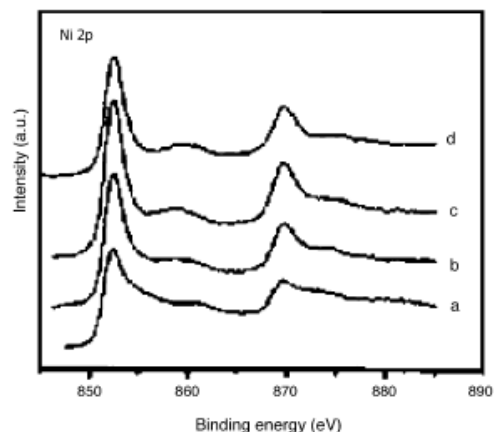


Fig. 1. (d)

Fig. X-ray photoelectron spectra of: 2, 6, 8 and 10 mol% Ni-doped TiO₂ thin films.

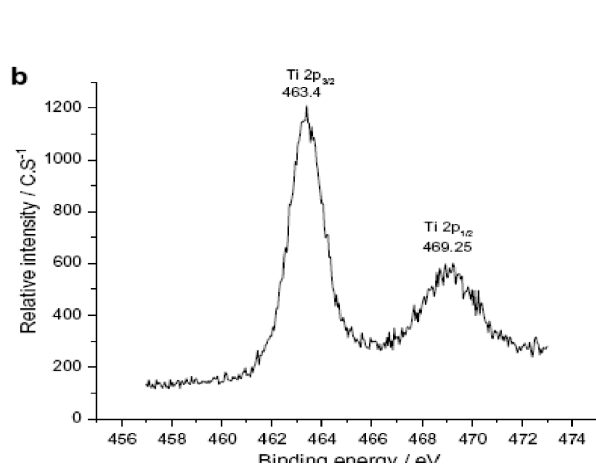


Fig. 1. (e)

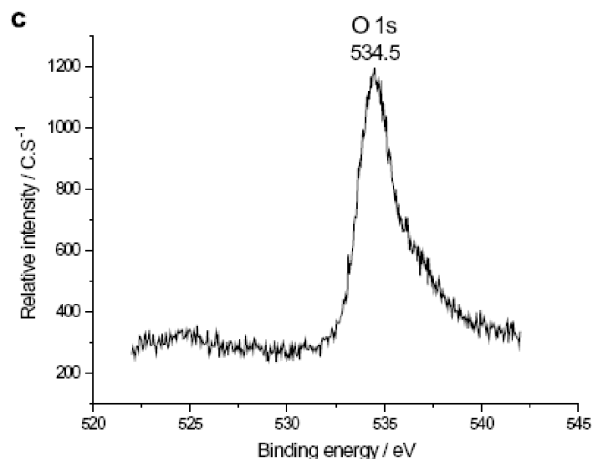


Fig. 1. (f)

The presence of NiO characterized by high-intensity satellites at the binding energy 9 eV higher than the main Ni 2p_{3/2} and Ni 2p_{1/2}. In samples c and d with higher Ni concentration, the Ni 2p peaks and their satellites had high intensity, indicating the existence of fully oxidized nickel oxide in the films [25]. Although the intensities of Ni 2p peaks were low because of the small amount of Ni, the shake-up satellites peaks with comparably high intensity could clearly be seen in the spectra. To a great extent, the final composition of the films depends not only on the chemical composition of the solution, but also on their intensity of hydrolysis and polycondensation processes, as well as on the substrate [26]. Fig. 1(e) and 1 (f) show the peak positions of Titanium and oxygen respectively.

3.3 Dielectric constant of Ni doped TiO₂ films

There are two modes of measurements i.e series mode and parallel mode [27]. The data of dielectric constant and D loss recorded in the parallel measurement mode. The dielectric constant was calculated from the knowledge of capacitance (C), film thickness (d), free space charge permittivity (ϵ_0) and area of the capacitor using the following relation.

$$\varepsilon = \frac{C_m}{C_0}$$

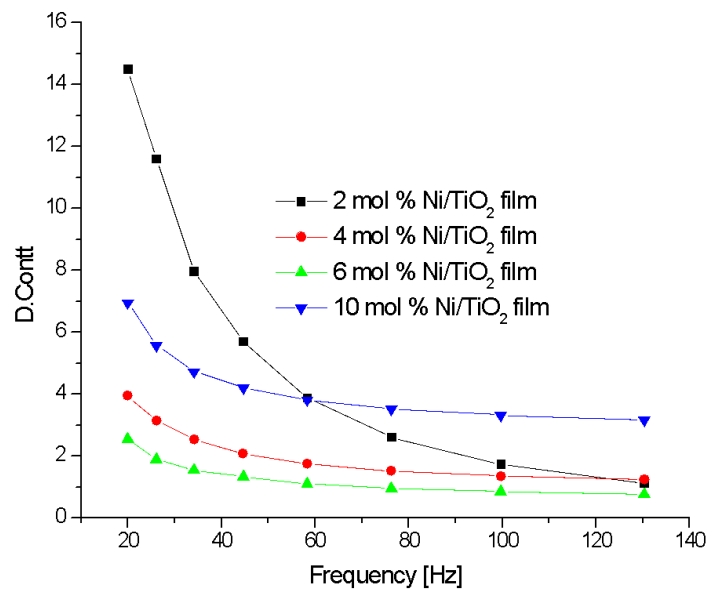


Fig. 2: Dielectric constant Vs frequency

Fig. 2 shows the graph of dielectric constant Vs frequency. It is clear from the graph that dielectric constant decreases with increase in frequency. It decreases also with an increase in Ni concentration. These curves closely resemble those predicted by the Debye's relaxation model for orientation polarization [28]. A saturation effect is observed In high frequency region, electric capacitance & dielectric constant are no longer frequency dependent. Dielectric constant depends upon various factors such as temperature, frequency of electric field, humidity, radiation effect, mechanical stress. The variation of dielectric constant with crystallite size may be expressed as follows. The defect sites in the TiO₂ lattice can induce defect oriented polarization to the neighboring defect free cells in the crystal lattice. This defect oriented polarization possesses short range ordering inside the lattice contributing to the total polarization of the TiO₂ lattice and therefore the total dielectric constant of the TiO₂ [29]. The growth of the microscopic Polar regions will be restricted due to the constraints for small crystallite sizes. As the crystallite size increases it enhances the growth of microscopic polar regions inside the crystallite and hence the dielectric constant with further increase of crystallite size the relative number of microscopic polar regions may be reduced due to larger crystallite sizes or it may be due to the loss of short range ordering due to larger crystallite sizes. An increase in frequency of the AC applied voltage decreases the value of dielectric constant of non linear dielectrics. The high dielectric constant at low frequency could be due to the presence of defective species such as Ti⁺³, electrode polarization or space charge injection [30-31] The very low value of dielectric constant at high frequencies is important for the fabrication of materials towards ferroelectric, photonics and electro-optic devices [32].

3.4 Dielectric Loss

Fig. no. 3 shows the d.loss of Ni doped TiO₂ films in the frequency range from 20 Hz to 10 MHz. The dissipation factor D, for the capacitor is normally composed of three parts: the actual series

resistance, the leakage resistance and the dielectric loss. Leakage resistance is responsible for the growth of dissipation factor at low frequency while the series resistance is responsible for the growth of d.loss at high frequencies. The value of d.loss decreased with increase in frequency and with increase in Ni content. The presence of dielectric loss peak in the sample is indicative of the dipolar relaxation processes.

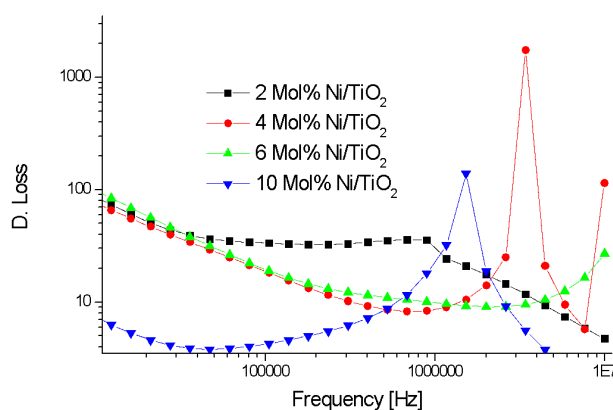


Fig. 3: D. loss for Ni/TiO₂ films

The behavior observed in dielectric loss with increasing frequency could be explained due to Maxwell-Wagner effect. Various factors such as thickness of the film, applied electric field, frequency of measurement, temperature affect the value of dielectric constant as well as d.loss. Oxygen vacancies distort the main structure unit of TiO₂ crystal, causing the appearance of additional electric dipole moments [33]. Dielectric loss occurs due to the heating effect of the dielectric material. D.loss in real materials the polarization does not respond instantaneously to an applied field. This causes d.loss. The origin of d.losses is the time delay between electric field and electric displacement values. D.losses increase with increase in number of grain boundaries per unit volume in new crystalline materials because grain boundaries are defective regions and suppress the harmonic oscillations of dipolar under an electric field.

The dielectric loss of any material describes qualitatively dissipation of electrical energy due to different processes i.e. 1) Dielectric conduction, 2) Dielectric resonance, 3) losses from non linear processes. Also the dielectric loss of various types are ion migration losses, DC conduction losses, ion jump and deformation losses ion vibration and electron polarization losses. Higher conductivity also favors the d.loss.

3.5 Density of interfacial states

We have calculated the number of interfacial states of pure and Ni doped TiO₂ thin films by using the formula [34] given by equation number (1) by taking capacitance at 20Hz and 10 MHz. In this Ni doped TiO₂ films the numbers of interfacial density of states with increase in Ni content are given in table 1.

$$N_{IS} = \frac{C_{LF} - C_{HF}}{e} \quad (1)$$

Table 1: Density of interfacial states of Ni doped TiO₂ films

Sample	Number of interfacial states(cm ⁻² eV ⁻¹)
2 mol % Ni/TiO ₂ film	0.749959X10 ¹¹
4 mol % Ni/TiO ₂ film	2.180125X10 ¹¹
6 mol % Ni/TiO ₂ film	1.33971875X10 ¹¹
8 mol % Ni/TiO ₂ film	3.5105625X10 ¹¹
10 mol % Ni/TiO ₂ film	1.582275X10 ¹⁰

IV. DISCUSSION

All the Ni doped TiO₂ thin films have been prepared by optimized sol-gel dip coating method. The particle size decreases with increase in Ni content. XPS studies confirmed that titanium exists in Ti⁴⁺ state in undoped and doped TiO₂ thin films. The binding energy peaks are observed at 534.5 eV, 463.4 eV and 289 eV respectively, which correspond to Oxygen, Titanium and Carbon respectively. The decrease in dielectric constant and dielectric loss with increase in frequency is due to decrease in particle size. Dielectric constant of the materials is the basic property which gives detailed information about polarization mechanisms. The very low value of the dielectric constant at higher frequencies is important for fabrication of materials towards ferroelectric, photonics and electro optics devices.

ACKNOWLEDGEMENT

This Research work was carried out on the joint collaborative research project (Project Number CAP15/KU/01) between National Physical Laboratory New Delhi (India) and Kurukshetra University Kurukshetra, Haryana (India). The authors are thankful to Director National Physical Laboratory New Delhi, India for providing the research facilities, encouragement, inspiration and discussion, The Authors are also thankful to Dr. Poonam, Assistant Professor, Govt. Post Graduate College Faridabad, Haryana (India) for her help in this work..

REFERENCES

1. Diana Mardare, G. I. Rusu, Materials Science and Engineering: B, Vol. 75(1), pp. 68, 2000.
2. J. Domaradzki, D. Kaczmarek, A. Borkowska, Physica Status Solidi, Vol. 205, issue 8, pp.1967, 2008.
3. Ming jing, Rujin Hang, Wen Shao, Hui Lin, Dawei Zhang, S. Songlin Zhuang, Daohua Zhang, Research Article, Vol. 25, pp.24, 2017.
4. S. Phadke, J.D. Sorge, S. Hachtmann, D. P. Birnie, Thin Solid films, Vol. 518, pp.5467, 2010.
5. M. C. Sehkar, P. Kondaiah, G. M. Rao, Svj Chandra, S. Uthanna, SuperLattice Microstructure, Vol. 62, pp. 68, 2013.
6. P. H. Wo Bekenbey, T. Ishwra, J. Nelson, D.D.C. Bradely, S. A. Hayue, T.D. Anthopoulos, Appl. Phys. Lett. Vol. 96, pp. 082116, 2010.
7. S. Aksoy, y. Caglor, J. Alloys Compounds, Vol. 613, pp. 330, 2014.

8. M.I Khan, Umar Farooq, Results in Physics, Vol. 7, pp. 2485, 2017.
9. N.D.M Said, M.Z. Sahdan, A. Ahmad, I. Senain, A.S. Abdullah, M. S. Rahim, AIP Conference Proceedings, Vol. 1788, pp. 030130, 2017.
10. Liu Lu, X.H Xia, Guosheng Shao, Jikui Luo, Journal of Physics D Applied Physics, Vol. 45, pp. 2012.
11. Sigrid Douven, Julien G. Mohy, Cedric Wolfs, Charles Reyserhove, Dirk Poelman, Francolis Devred, Eric M. Gaigneaux, Stepharnie D. Lambert, Journal of Catalysts, Vol. 10(5), pp. 547, 2020.
12. D. Mardare, G. I. Rusu, J. of Optoelectronics and Advanced Materials, Vol. 6, pp. 333, 2004.
13. Iulia Salaoru, Themistoklis, Prodromakis, Ali khiat, Christofer Toumazou, Applied Physics Letters, Vol. 102, pp. 013506, 2013.
14. Davinder Singh, K.K. Saini, London Journal of Research in Science Natural and Formal, Vol. 19, 2019.
15. Davinder Singh, Alka Singhal, Neenu Saini, Journal of Scientific Research in Physics and Applied Sciences, Vol. 7, pp. 35, 2019.
16. Massimo Tallarida, Chittranjan Das and Dieter Schmeisseer Beilstein, Journal of Nanotechnology, Vol. 5, pp. 77, 2014.
17. Y. Shi, X. W. Wang, T. P. Ma, IEEE, Trans electron devices, Vol. 46, pp. 362, 1998.
18. Y. Uu, H. Niimi, H. Yang, G. Lucovsky, R. B. Fair, j. Vac, Sci. Technol. B, Vol 17, pp. 1813, 1999.
19. B. De Salvo, Ghibaudo, G. Pananakakis, B. Guillaumot, G. Reibold, Journal Applied Physics, Vol. 86, pp. 2751, 1999.
20. Y. wu, Y. M. Lee, G. Lucovsky IEEE, Electron Device Lett. Vol. 21, pp. 216, 1999.
21. Davinder Singh, Nafa Singh, Sunil Dutta Sharma, Chander Kant, C.P. Sharma, R. R. Pandey, K. K. Saini, Journal of Sol-gel Science and Technology, Vol. 58, pp. 269, 2010.
22. Sunil Dutta Sharma, Davinder Singh, K. K. Saini, Chander kant, Vikash Sharma, S. C. Jain, Applied catalysis A, Vol. 314, pp. 40, 2006.
23. P. Indra Devi, K. Ramachandran, Journal of Experimental Nanoscience, Vol. 6, pp. 281, 2011.
24. A. Fujishima, T. N. Rao, D.A. Tryk, Journal Photochem Photobiol, C1, 1, 2000.
25. G. H. Yu, C. L. Chai, F.W. Zhu, J. M. Xiao, W. Y. Lai, Appl. Phys. Lett. Vol. 78, pp. 1706, 2001.
26. Ch. Trapalis, V. KOzhuharov, B. samurneva, , P. Stefanov, Journal Material Science, Vol. 28, pp. 1276, 1993.
27. B. Karunakaran, S. J. Chung, E. K. Suh, D. Mangalaraj, Physica B: Condensed Matter, Vol. 369, pp. 129, 2005.
28. H. Birey, Journal Applied Physics, Vol. 49, pp. 2898, 1978.
29. D. Pamu, K. Sudheendran, M. Ghanshyam, K. C. James Raju, Anil K. Bhatnagar, Vacuum, Vol. 81, pp. 686, 2007.
30. J. Y. Kim, H. S. Jung, J. H. No, J. R. Kim, K.S. Hong, Journal Electroceramics, Vol. 16, pp. 447, 2006.
31. G. A. Kontos, A. I. Solunitizis, P. K. Karahaliou, G.C. Psarras, S. N. Georgia, C.A. Krontiras, . N. Pizaniias, Express Polym. Lett. Vol. 1, pp. 781, 2007.
32. R. Rajeswari, D. Venugopal, International journal of Creative Research thoughts (IJCRT), Vol. 6, pp. 683, 2018.
33. Valentine Bessergenov, Materials Research Bulletin, Vol. 44, pp. 1722, 2009.
34. H. Tavakolian, J.R. Sites, Proceedings, of the 20th IEEE photovoltaic specialists conference, NV, IEEE, New York, 1608, 1988.



Scan to know paper details and
author's profile

Etiological Aspects of Fusarium Corn Stalk Rot Under the Cold Tropic Conditions

*Germán Maldonado-Archila, Gustavo Ligarreto-Moreno, Sandra- Melo Martinez
& Sandra Gómez -Caro*

Universidad Nacional de Colombia

ABSTRACT

Since 2017 corn crops (var. Simijaca) that are adapted to cold climate production zones in Colombia has been affected by Stalk Rot with an incidence up to 40% which is caused by *F. graminearum* and *F. subglutinans*. This study aimed to determine the sources of *Fusarium* spp. inoculum and evaluate the effect of management of potential Inoculum on disease, plant growth and crop yield, and to relate the preponderant climate and landscape conditions with the disease. Two plots were selected for the study, one with corn-corn crop sequences where the crop residues were kept or removed, and the other with a rotation scheme including zucchini (*Cucurbita pepo*). The corn seeds were treated with wet and dry heat at different temperatures and evaluate in join with residues management as measures of the disease control. *Fusarium* inoculum were detected on stand corn crop residues, detritus on the soil, air and seeds.

Keywords: *zea mays* l., fusarium stalk rot, cold tropic, crop residues management, heat seeds treatment, climate variability, crop fitness.

Classification: LCC: S

Language: English



Great Britain
Journals Press

LJP Copyright ID: 925693

Print ISSN: 2631-8490

Online ISSN: 2631-8504

London Journal of Research in Science: Natural and Formal

Volume 23 | Issue 9 | Compilation 1.0



© 2023. Germán Maldonado-Archila, Gustavo Ligarreto-Moreno Sandra-Melo Martinez & Sandra Gómez -Caro. This is a research/review paper, distributed under the terms of the Creative Commons Attribution-Noncom-mercial 4.0 Unported License <http://creativecommons.org/licenses/by-nc/4.0/>, permitting all noncommercial use, distribution, and reproduction in any medium, provided the original work is properly cited.

Etiological Aspects of Fusarium Corn Stalk Rot Under the Cold Tropic Conditions

Germán Maldonado-Archila^a, Gustavo Ligarreto-Moreno^o, Sandra- Melo Martinez^p
& Sandra Gómez -Caro^{co}

ABSTRACT

Since 2017 corn crops (var. Simijaca) that are adapted to cold climate production zones in Colombia has been affected by Stalk Rot with an incidence up to 40% which is caused by *F. graminearum* and *F. subglutinans*. This study aimed to determine the sources of *Fusarium* spp. inoculum and evaluate the effect of management of potential Inoculum on disease, plant growth and crop yield, and to relate the preponderant climate and landscape conditions with the disease. Two plots were selected for the study, one with corn-corn crop sequences where the crop residues were kept or removed, and the other with a rotation scheme including zucchini (*Cucurbita pepo*). The corn seeds were treated with wet and dry heat at different temperatures and evaluate in join with residues management as measures of the disease control. *Fusarium* inoculum were detected on stand corn crop residues, detritus on the soil, air and seeds. The results indicated that crop rotation, crop residues removal, and heat treatments on the seed were effective strategies for managing the disease. Crop rotation showed the highest growth values, while seed treatments with dry heat at 50°C under crop rotation showed the lowest incidence and lodging, However, regarding yield, crop rotation reduced to the middle the number of ears despite the fact that higher growth values were obtained, highlighting the importance of the association of corn of the regional variety Simijaca (var. Simijaca) with *F. graminearum* and *F. subglutinans*. The obtained results allowed the holistic understanding of corn lodging and provided insights for the design of disease management strategies for corn production systems in cold weather in the tropics.

Keywords: zea mays l., fusarium stalk rot, cold tropic, crop residues management, heat seeds treatment, climate variability, crop fitness.

Author ^a ^o ^p ^{co}: Faculty of Agricultural Sciences, Department of Agronomy, Universidad Nacional de Colombia, Bogotá, Cundinamarca, 111321, Colombia.

I. INTRODUCTION

Corn is one of the bases of planetary food security. It is the second most important crop after wheat (Paliwal, 2016) and Colombia is the fourth largest producer in South America being the third crop most sown in the country (CIAT & CIMMYT, 2019). In recent years, corn crops in the municipality of Simijaca at the Ubaté valley have been affected by Stalk Rot caused by *Fusarium graminearum* in the *Fusarium graminearum* species complex (FGSC) and *Fusarium subglutinans* in the *Fusarium fujikuroi* species complex (FFSC) (Maldonado et al., 2022). Although *Fusarium* Stalk Rot (FSR) is among the most economically important diseases of corn around the world (Wang et al. 2017 and Yang et al. 2010) it is not a frequent disease in Colombia and had not been reported for at least 30 years in Cundinamarca (Buritica, 1999; Maldonado et al., 2022).

Fusarium spp. produce wide spore's variety on crop residues that are transported through atmosphere and disseminated by means of air, raindrops, insects and seed which is infected trough pistils (Duncan

and Howard, 2010; Munkvold et al. 1997; Ooka and Kommedahl, 1977; Windels et al. 1976). *Fusarium graminearum* (FGSC), *Fusarium verticillioides* (FFSC) y *Fusarium proliferatum* (FFSC) entry in the corn plant through trichomes, leave xylem and stem (Nguyen et al. 2016; Nguyen et al. 2015) and given that spores are passively transported by the wind, any landscape characteristic influence their movement and impact their deposition (Plantegenest et al. 2007, Schmale et al. 2006).

There is evidence of *Fusarium* spp. endophytes in wild and cultivated plants and the best example is *F. verticillioides*. In this case, *F. verticillioides* is associated with corn plants along the complete crop cycle, where the plant responses to the infection depend on several factors related to plants, fungi, and environment (Kuldau & Yates, 2000). The endophyte state is transient and *F. verticillioides* switches from an asymptomatic and biotrophic lifestyle to an hemibiotrophic one causing disease (Schulz et al., 1999). Stress conditions promote the disease onset and a range of virulence can be observed among different strains. However, strains that can be pathogenic are known to be asymptomatic under optimal plant growth conditions (Kuldau & Yates, 2000).

Thermal stress (cold and heat), drought, high sowing density, shadow, pest attacks and the use of fertilizers with high nitrogen and low potassium content are examples of stress conditions that can promote disease on a very well-balanced association between the plant and *F. verticillioides* (Dodd, 1980a; Schulz et al., 1999; Kuldau & Yates, 2000; Blandino et al., 2009). The theory of photosynthetic balance between stress and translocation could be explain and unify the triangle of disease, this theory mentione that if a stress source is aplicated under specific environmetal conditions, corn plant will develop Stalk Rot and favor one of the multiple fungi that are ubicous and have the potential to cause disease (Dodd, 1980a).

Interest on no tillage and multiple crops has increase in the last two decades' due concern about erosion soil and lack of food and fuel supply (Cotten and Munkvold, 2007). Although in some cases no tillage practices reduce diseases severity, in other cases the epidemics enhance (Broders et al. 2007). Corn crop residues typically has been considered a key source of inoculum of several phytopathogenic fungi including *Fusarium* spp. enhancing their disease incidence under minimum or no tillage schemes. For example, in the case of *Fusarium verticillioides*, *F. proliferatum*, and *F. subglutinans* (FFSC) corn crop residues act as source of long term (630 days) for the corn plants infection under corn monoculture and corn/soybean/oat rotation scheme (Cotten and Munkvold, 2007).

Due the fact that *Fusarium* spp. produce wide spore's variety on crop residues which serve as source of inoculum to the horizontal transmission, the burial of crop residues to destroy phytopathogens is an ancestral agricultural practice to reduce the inoculum levels of inoculum in the soil to prevent their emergence and decomposition which can help to prevent disease spread (Drayton, 1929). However, although Management of crop residues is suggested as a disease control measure in corn, there is little evidence convincingly demonstrating the success of this approach (Sumner et al. 2003) and until now the relationship between crop residues and diseases remain unclear (Cotten y Munkvold, 2007).

Fusarium spp. can infect the corn seeds through both horizontal and vertical transmission. Vertical transmission occurs when the seeds come from plants that are already infected, while horizontal transmission occurs when the spores are transported by air and infected the pistils of the corn plant, leading to seed infection, which can act as a source of inoculum for the next crop, which can lead to the perpetuation of the disease cycle (Duncan and Howard, 2010; Machado et al. 2003; Munkvold et al. 1997). Therefore, proper management practices, such as seed treatment and selection of healthy seeds are crucial in reducing the impact of *Fusarium* spp. on corn crops.

There are several studies about heat treatments to control *Fusarium* spp inoculum on seeds, where for example dry heat treatment on wheat and barley eliminate completely *F. graminearum* inoculum

without germination reduction and similar positive results have been reported for the thermal treatment of corn seeds and other cereals (Clear et al., 2002; Coutinho et al., 2007; Bennett & Colyer, 2010; Piñeros-Guerrero et al., 2019).

Given the recent problem of corn lodging caused by Stalk Rot in high-altitude corn-producing regions of the Ubaté Valley of Colombia, the objectives of this study was to determine the principal inoculum sources of *Fusarium* spp. in the field, the effect of management of the potential of *Fusarium* spp. inoculum on parameters disease, plant growth and crop yield and relate the preponderant climate and landscape conditions present in the municipality of Simijaca during 2017 with the disease reports, when “El Niño” episode occurred in the zone of study.

II. MATERIAL AND METHODS

Source's inoculum of Fusarium spp.: samples of seeds of the regional variety Simijaca, detritus on the soil, crop standing residues, spore in the air and soil were collected from two plots with stalk rot history located in the municipality of Simijaca (Cundinamarca, Colombia) (5°N 29' 49'', -73°W 49' 55'' and 5°N 33' 11'', -73°W 47' 29''). The detritus was collected with a sieve with 1,0 mm in size, the spore capture was performed for 12 h at the night on slant with emended media (Prussin, 2013). *Fusarium* spp. isolation from the seeds, detritus and crops standing residues were achieve using 3% Agar (30 g L⁻¹) (Oxoid ®) and Potato Dextrose Agar emended with 2-Benzoxalolinone (PDA-BOA) (Glenn et al. 2002) and 12 mL⁻¹ Chloramphenicol and 20 mL⁻¹ (Leslie & Summerell, 2006). BOA preparation was in absolute ethanol and added in the medium after autoclaving and cooled to 50°C. The doses were adjusted to 0,33 g of BOA per liter of medium and all isolates were incubated at 25°C in dark conditions (Model FD 23, BINDER, Germany). Finally, the inoculum presence in the soil was evaluated by dilution standard on base 10 from 100 g of soil on PDA medium (Leslie & Summerell, 2006).

Effect of Fusarium spp. on the corn stem lignification: seeds of the regional variety Simijaca (var. Simijaca) treated with wet heat at 52°C and without treatment were sown on soil from a non-agricultural area in the Bogotá plateau (soil inoculum free) and from commercial corn crops with stalk rot history in the municipality of Simijaca (soil naturally infested by *Fusarium* spp.). The inoculum presence in the soil was ruled out by dilution standard on base 10 from 100 g of soil and plated in PDA-BOA as mentioned above. The trays were maintained by 30 days (V3) in greenhouse conditions (+/- 25°C) and then, transversal cuts of the base of the stem were freehand obtained, a drop of Weisner staining was put on microscope slide, the stem cut put on in and examine under microscope (CX 31, Olympus, Japan) (Yates et al. 1997). Weisner staining was prepare immediately before of the evaluation (Pradhan and Loqué, 2014).

Climatic and landscape conditions and their relationship with corn stalk rot events in the Ubaté valley: climatic data for 30 years (1986-2016) for the municipality of Simijaca were collected from “Corporación Autónoma Regional de Cundinamarca (CAR)” and establish a base line for month for precipitation (mm), relative humidity (%), wind speed (m/s), maxim, minim and average temperature (°C). These data were compared with the registered in two experimental plots located in the Simijaca municipality in Cundinamarca (5°N 29' 50'', -73°W 49' 47'' y 5°N 29' 41'', -73°.49' 17'') through climatic station iMETOS ® 300 (Pessl instruments, Weiz, Austria) with measure each 10 min and data viewed in real time. Precipitation, wind speed, minim temperature and number hours with temperatures below 10°C were calculated daily from May 2016 to July 2017 and related with landscape conditions and corn stalk rot and lodging reports in commercial corn crops in the study zone.

Effect of management of the inoculum potential of *Fusarium graminearum* and *Fusarium subglutinans* on parameters of disease, plant growth, and crop yield of cold-climate corn (*Zea mays* L.) crops under Ubate valley conditions.

Heat treatments to the corn seed of the regional variety Simijaca: one day before experimental set up in the field, corn seeds of the regional variety Simijaca (var. Simijaca) were put in tap water for four hours, then the seeds were heat treatment at 50 °C, 55°C and 60°C through their exposition to dry heat (Bennett and Colyer, 2010) in a heat chamber (Model FD 23, BINDER, Germany) or wet heat (Daniels, 1983) in an evaporator (Waterbath B-480, BÜCHI Labortechnik AG, Switzerland). Under dry heat at 50°C, 55°C, 60°C and wet heat at 50°C the exposition time were 10 minutes; under wet heat at 55°C and 60°C time exposition was for 5 minutes. This study considered seeds without any treatment as absolute control.

Chemical control used by farmers: as commercial treatment we evaluated the seed's chemical treatment used by the farmers based in the mixture of active ingredients thiabendazole (0,2 g de i.a /Kg), metalaxil + propamocarb (5,0 g de i.a /Kg), oxytetracycline hydrochloride + gentamicin sulfate (2,0 g de i.a /Kg) and carboxim + thiram (4,0 g de i.a /Kg). This treatment was used by the farmers due to the inaccurate diagnosis of the disease at that moment and oriented to management the seed borne inoculum of bacteria, fungi and oomycetes.

Crop rotation and corn crop residues management: seeds treatments mentioned above were taken to the field in two localities in the Simijaca municipality (Cundinamarca, Colombia) (5°N 29' 50'', -73°W 49' 47'' and 5°N 29' 41'', -73°.49'17''). The first plot evaluates crop rotation (480 m²) without corn sowing in at least two years and where the last crop was zucchini (*Cucurbita pepo*). The second plot evaluates corn monoculture for at least two years in a plot (960 m²), which was divided in two: the half with corn crop residues remotion and the other half where the crop residues were kept it.

Agronomic management: each treatment was sown in 15 m² and the management in the experimental plots was the usually employed by farmers in the zone of study and just the chemical fertilization was fractionated in three applications during vegetative crop stages at V3, V6 and V9. Distance between lines was of 0,9 m and between plants 0,5 m (22000 plants ha⁻¹). From experimental plots soil samples were taken a 30 cm in depth for chemical and textural analyses.

Variables: one month after sowing the stand establishment for each treatment was determinate. Monthly, height from the stem base up to tassel of five plants (m), the stem base diameter (mm) of 10 plants, stalk rot incidence (%) (considering plants that showed chlorosis, anthocyanosis and dwarfing symptoms) and the lodging (%) was evaluated. Dates coincided with development stages of V3, V6, V9, VT, R1 (Ritchie et al. 1996). The yield in terms of number and weight ears (Kg), ear number per plant, and weight of 10 ears (Kg) were determinate at harvest, five months after sowing when the grain was milky with 40% dry matter (R4).

Experimental design: experiment was developed under a split-plot design with three plots corresponded to crop rotation and the scheme of crop residues management (removed or kept) and eight subplots (heat and chemical seeds treatments plus the absolute control). The experiment had four repetitions and one replicate and the time was blocked (except for lodging). The stand establishment, number and weight of ears; and number of ears per plant were subjected to variance and normality tests and compared under Tukey's 0.05 significance. Stem diameter and lodging data was transformed by square root, plant height by potency 0.07 and stalk rot incidence by natural logarithm. Once the data was transformed were subjected to variance and normality test and compared under Tukey's 0.05 significance. Data analysis was performed using SAS v 9.4 (SAS Institute, Cary, NC, USA) and graphics shows untransformed data.

III. RESULTS

Epidemiological aspects of Fusarium graminearum and Fusarium subglutinans under Ubate valley conditions and their relationship with corn

Inoculum Sources of Fusarium spp. inoculum of *F. graminearum* was detected in standing crop residues (100%), air (100%) and seeds (4%), whereas *F. subglutinans* inoculum was found in detritus present in soil (100%) and seeds (5%). Highlighting the *Fusarium* spp. absence in the soil.

Effect of Fusarium spp. on the corn stem lignification: at histological level, plants grown in absence of *Fusarium* spp. showed lower qualitative content of lignin respect plants grown with some source of inoculum from the seed or soil. Plants grown in absence of inoculum had a normal stela distribution and the Weisner stain stained the vessel xylem. Plants with inoculum from seed or soil showed higher lignin content in form of an external ring of lignin in the stem. Additionally, plants from seeds without heat treatment (endogen inoculum) had higher number of adventitious roots which were pink stained by phloroglucinol (Fig. 1).

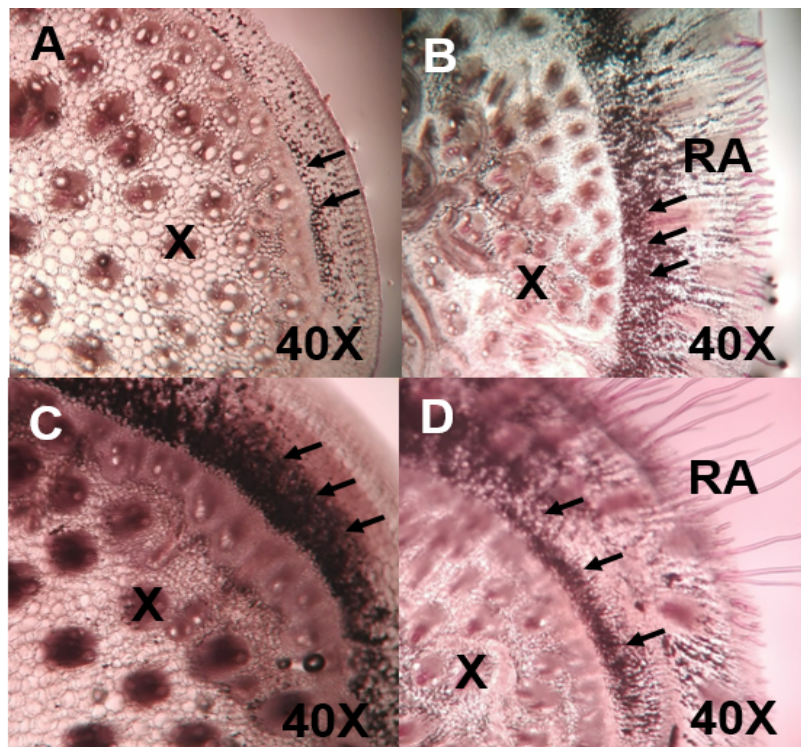


Figure 1: Effect of *Fusarium* spp. inoculum on corn stem lignification in the Simijaca variety (var. Simijaca) 35 days after sowing and evaluated by Weisner staining. A) plants without inoculum on seed and soil. B) plants from seeds naturally infected and grown on soil free of inoculum. C) plants from seeds treated with heat and grown on soil naturally infected. D) Plants from seeds naturally infected and sown on soil naturally infected. X: xylem; RA: adventitious roots. The rows indicate the lignin accumulation in the extern part of the stem in ring form.

Climatic and landscape conditions and their relationship with corn stalk rot events in the Ubate valley: land scape of Simijaca corresponded to a valley and climatic conditions during 2016 and 2017 were influenced by a tropical “El Niño” event. Average temperature during 2016 was 13,2°C, with a humidity relative of 81% and precipitation of 429 mm (Figure 2). Precipitation record between May until December 2016 were lower in 125 mm respect historical records for thirty years in the zone (554

mm) (Figure 2a). On another hand, 2017 had an average temperature of 13,4°C, humidity relative of 88% and precipitation of 670 mm between January until September 2017 (the precipitation level registered was higher in 74 mm respect the historic of 596 mm). Humidity relative for both years (Figure 2b) was superior to the historic data because to a marked reduction in the wind speed (Figure 2f). Nevertheless, from June to September 2016 the ambient was dry (HR< 80%). Average maximum temperature calculated for each month was superior respect with historic (Figure 2c). the average minimum temperature showed a gradual diminution from 9°C to 5°C from May to September 2016 and a diminution from 9°C to 5°C in February 2017 and 9°C to 8°C in April 2017 (Figure 2d). Maxim temperatures were slightly superior and minimum temperatures were inferior to the historic indicating a mayor thermic amplitude reflected in terms of temperature's delta (Figure 2e). In the study zone, temperature's delta historic corresponded to 10°C, which was inferior respect to 13,4°C registered from May to September 2016 and the 12,8°C registered from February to August 2017. In Figure 3 is shown episodes of high intensity cold stresses monthly from May 2016 to August 2017 in there the high number of high intensity cold stresses during July and August 2016 presented in the Ubate valley when corn crops were on reproductive phase determinate late lodging, conversely, high intensity cold stresses presented during September 2016 when corn crops in the zone were on vegetative phase determinate early lodging.

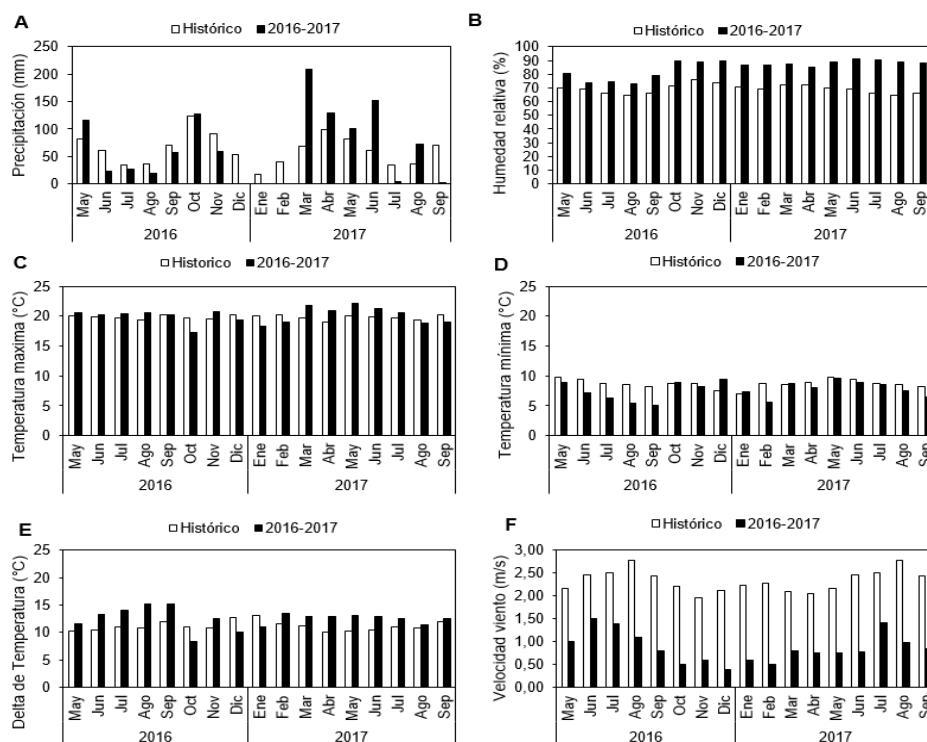


Figure 2: Behavior of climatic variables from May 2016 to September 2017 in the municipality of Simijaca, Cundinamarca with respect to historical data of 30 years for this location. A) accumulated precipitation per month. B) average relative humidity per month. C) Average of maximum temperature per month. D) average of minimum temperature per month. E) delta of temperature calculated as the difference between the maximum and minimum temperature and F) average wind per month.

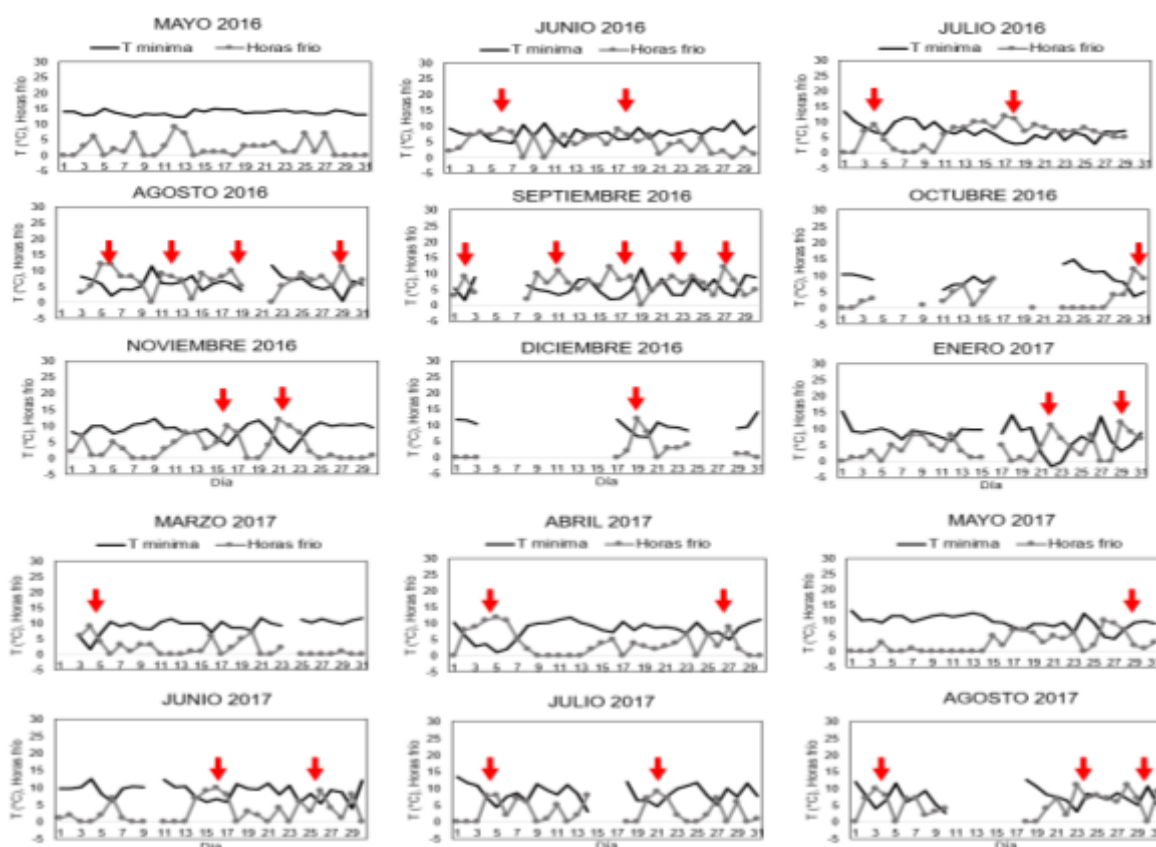


Figure 3: Behavior of the minimum temperature and cold hours per day from May 2016 to August 2017 in the municipality of Simijaca, Cundinamarca. The red arrows indicate events of high intensity cold (minimum temperature below 10°C for more than ten hours). Weather data were obtained with iMETOS® weather stations in commercial corn plots.

Effect of management of the inoculum potential of Fusarium graminearum and Fusarium subglutinans on parameters of Stalk Rot of tropic cold-climate corn (Zea mays L.) crops under Ubate valley conditions.

Respect to stalk rot incidence, disease had a monocyclic behavior (Figure 4a). Crop rotation for at least 24 months reduced the stalk rot incidence ($P=0,0376$). Although there not significance statically difference between remove or kept corn crop residues, when they are removed, lower incidence values were observed. At V6 development stage, stalk rot incidence was similar between plots evaluated, while at V9 and VT (tasseling) stages, higher incidence was registered in corn monoculture when the residues are kept, intermediate ones when are removed and lowest under crop rotation. In silking (R1), incidence was similar between three plots again (Figure 4b).

On another hand, chemical seed treatment had the highest incidence (19%) and dry heat treatment at 50°C the lowest (13%) ($P=0,0022$) the rest of treatments were intermediate (Figure 4c). Most of seed treatments under crop rotation scheme had lower incidence respect corn monoculture with or without residues in the surface (Table 1). Seeds with heat treatment with dry heat at 50°C and wet heat at 60°C always that were sown in crop rotation scheme reduce the stalk rot incidence ($P=0,0022$). Seeds treated at 60°C in the monoculture scheme with crop residues had the highest incidence.

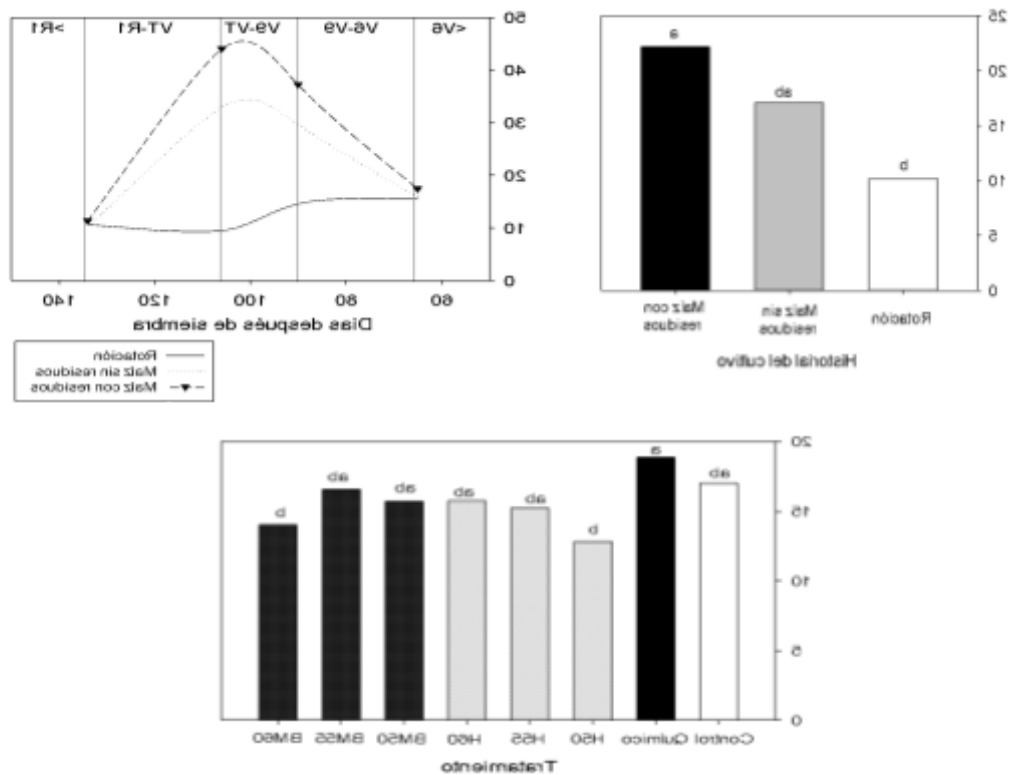


Figure 4: Corn Stalk Rot of the regional variety Simijaca under three rotation schemes and residues management. A) disease incidence behavior during development stage of 6 and 9 true leaves (V6, V9), tasseling (VT) and silking (R1). B) incidence according to rotation and residues management scheme. C) Corn Stalk Rot incidence at R1 development stage 140 days after sowing on plants from seed with heat treatment. H: dry heat; BM: wet heat at 50, 55 and 60 °C. Different letters indicate significance statistical difference according to Tukey ($p < 0,05$).

Regarding lodging it was detected from 90 DAS (V9) in low values and without statistical difference respect to tasseling (VT) however both evaluations dates (V9 and VT) were significantly different respect R1 and R4 ($P=0,0012$) (Figure 5a). At harvest point (R4), lodging was highest under monoculture scheme with corn crop residues left in the surface (41%), intermediate when the residues were removed (32 %) and the lowest under crop rotation (18%). Although without statistical difference ($P=0,2741$) trend was kept since silking (R1) until harvest (Figure 5b). Lodging at harvest point (R4) (Figure 5b) was close to the maximum incidence record in tasseling (VT) (Figure 4 b).

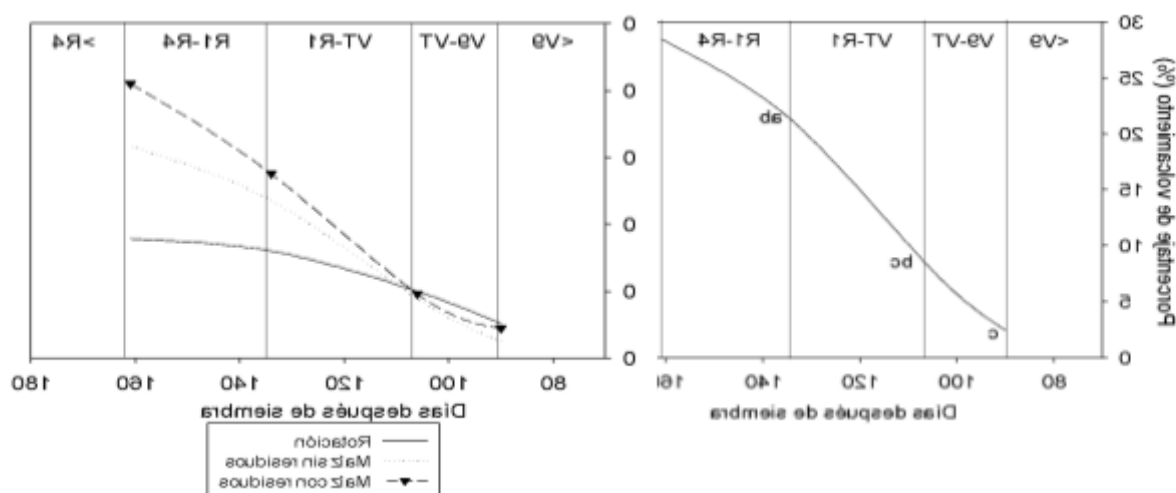


Figure 5: Behavior of lodging on the Simijaca variety (var. Simijaca) according to: A) the crop rotation and residues management scheme and B) the date of evaluation. (V6, V9): development stage of 6 and 9 true leaves, (VT): tasseling, (R1) silking and (R4) ears with 40% of dry matter. Different letters indicate significance statistical difference according to Duncan and Tukey ($p < 0,05$).

Seed treatments Individually had no effect on lodging ($P = 0,1343$), however seeds exposed to dry heat at 50°C and 60°C and sown under crop rotation scheme reduced it. In the same way seeds exposed to wet heat at 50°C and 55°C and sown under monoculture scheme where residues were kept enhance it ($P = 0,0122$) (Table 1). Seeds subjected to dry heat at 50°C and sown under crop rotation scheme showed low lodging values respect most of treatments, excluding the chemical and absolute control under monoculture scheme where corn crop residues were kept (Table 1). Seed treatment with dry heat at 50°C and 60°C sown under crop rotation scheme had a net reduction in 54% and 23% on lodging.

Table 1: Interaction between crop scheme, residues management and the seed heat treatments of the Simijaca variety (var. Simijaca) on the Corn Stalk Rot incidence and the percentage of lodging Different letters indicate significance statistical difference according to Duncan and Tukey ($p < 0,05$).

Historial del cultivo (parcela principal)	Tratamiento a la semilla (sub-parcelas)	Incidencia		Volcamiento	
		%		%	
Rotación	control	11,33	fg	11,87	abc
	quimico	17,54	abcde	13,77	abc
	H50	7,68	h	5,76	c
	H55	9,86	fgh	12,35	abc
	H60	8,90	gh	7,51	bc
	BM50	8,97	gh	12,78	abc
	BM55	12,16	efg	8,20	bc
	BM60	7,80	h	12,43	abc
Maíz sin residuos	control	17,80	abcd	14,04	abc
	quimico	16,23	cde	12,95	abc
	H50	13,40	def	10,79	abc
	H55	17,61	abcde	11,32	abc
	H60	19,43	abcd	11,33	abc

	BM50	19,51	abcd	11,73	abc
	BM55	17,23	abcde	15,19	abc
	BM60	16,43	bcde	13,79	abc
Maíz con residuos	control	24,38	ab	10,75	abc
	quimico	23,57	abc	15,15	ab
	H50	20,52	abc	16,95	ab
	H55	20,33	abc	16,66	ab
	H60	25,47	a	16,04	ab
	BM50	22,17	abc	19,04	a
	BM55	21,64	abc	19,63	a
	BM60	20,77	abc	15,44	ab

Effect of management of the inoculum potential of Fusarium graminearum and Fusarium subglutinans on growth and yield parameters of tropic cold-climate corn (Zea mays L.) crops under Ubate valley conditions.

Stand establishment were similar between crop rotation and monoculture scheme where crop residues were removed (64,2% and 64,3%) while under monoculture scheme with residues left on soil stand establishment was higher (68,5%) ($P=0,0413$) (Figure 6a). There was not statical difference between seed heat treatments and absolute control although chemical treatment showed the lowest establishment ($P<0,0001$).

Plant height and stem diameter as vigor measure at tasseling development stage were not affected by seed treatments (thermal or chemical) respect absolute control. Nevertheless, crop rotation scheme had the highest values of height (2.9 m) and stem diameter (33.9 mm) (Figure 6 b and c) respect to corn monoculture where the crop residues was removed (2.3 m and 25,98 mm) or kept it (2.2 m and 24,16 mm) ($P<0,0001$).

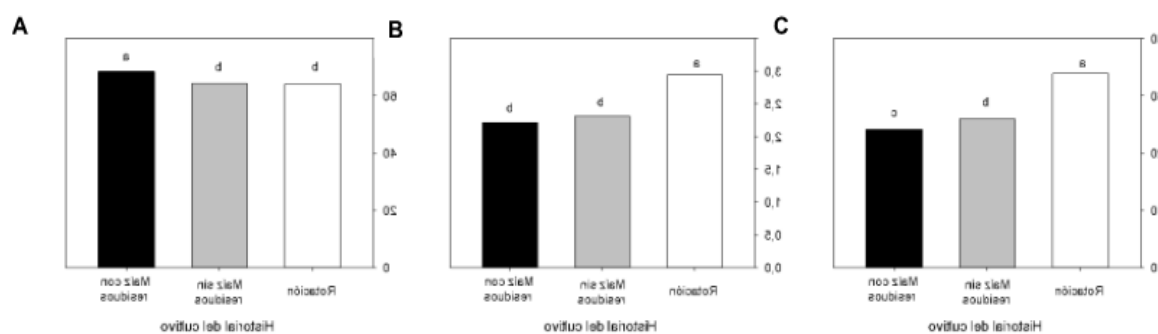


Figure 6: Effect of crop rotation and residue management scheme on: A) establishment percentage 30 days after sowing, different letters indicate significance statistical difference according to Duncan ($p<0,05$). B) plant height, C) stem diameter of corn of the Simijaca variety (var. Simijaca) 106 days after sowing at tasseling stage of development (VT), different letters indicate significance statistical difference according to Duncan and Tukey ($p<0,05$).

Regarding the number and weight of ears (Figure 7a and b) under corn monoculture scheme with or without residues remotion similar values obtained but duplicating obtained in crop rotation scheme ($P=0,0035$ and $P<0,0001$, respectively). A trend to obtain lower weight (2 Kg) was noted when the corn residues were kept it respect when were removed ($P=0,0068$). Statistical differences between

Given that *Fusarium* mycelium and spores resides on detritus and not form chlamydospores, inoculum was not detected from soil (Leslie and Summerell, 2006). The spores generated on all these inoculum source have been reported have the capacity to be transported by means of air as an effective dissemination way for aerial corn colonization through trichomes, leave xylem and stem (Nguyen et al. 2016; Nguyen et al. 2015) and given that spores are passively transported by the wind, any landscape characteristic influence their movement impact their deposition (Plantegenest et al. 2007, Schmale et al. 2006).

Simijaca is located in the middle of the Ubaté valley where mountains regulate cold air masses concentrating them in the low zones and allowing them to flow on the slopes and this landscape condition had epidemiological consequences regulating move of air masses and *Fusarium* inoculum dispersion, giving to the disease a localized behavior in the valley and scape zones on the slopes or other production areas. Increased lignin deposition observed in the stem of corn Simijaca grown in naturally infested soil with *Fusarium* spp. is accord with observations made for Yates et al., (1997) where differences on lignin synthesis of plants inoculated with *F. verticillioides* were observed. This could be a structural mechanism to prevent fungal growth within the corn stalk during the association (Borja et al. 1995; Irizarry and White, 2018; Vance et al. 1980).

Although in the recent epidemics of corn Stalk Rot at the Ubaté Valley were associated with *F. graminearum* and *F. subglutinans* (Maldonado et al., 2022), Dodd (1980a) stated that identification of the causal agent of disease in little contributes to its management and the host-environment interaction is the pertinent condition to analyze. Several environmental stresses have been associated with the occurrence of stalk rot (Blandino et al. 2009; Dodd, 1980a), among them, low temperatures for example reduce seed and plant metabolism and enhance disease risk. Temperatures below 10°C are the most prejudicial and damage will be greater in soil with poor drainage (Saab and Steve, 2006). In this work two climatic variables were found had a major impact on corn stalk rot in variety Simijaca: drought and minimum temperature.

In the Ubaté valley to higher precipitation lower corn lodging were reported. The cold viewed as minimum temperature and episodes of high intensity cold stresses (temperatures below 10°C up to six hours) were associated with corn stalk rot reports. How these two stress conditions affect also depends on the phenological state of corn in which it is affected. Therefore, more developed crops that are affected by drought and cold tend to lodging late in the crop cycle while young crops tend to lodging early.

Fusarium spp. is virtually associated with all modern corn varieties around the world however Stalk Rot not always is developed, this ancient and evolutive relationship can promote plant growth without affect seeds germination, protect the seed from infection by other 10 genera of fungi while the plant serves as a source of carbon and a pathway of vertical and horizontal transmission of the fungus (Van Wyck et al., 1988; Wicklow, 1988; Yates et al., 1997; Schulz et al., 1999; Kuldau & Yates, 2000). A protected and humid environment, safe source of nutrition and vertical and horizontal transmission mediated by plant would be benefits for the fungi (Kuldau and Yates, 2000).

Framed in the photosynthetic balance between stress and translocation proposed by Dodd, (1980a) the passage from a vegetative growth phase to reproductive one induces expression of the final symptom of lodging as were observe in this work, due stalk weakness and sink demand. Furthermore, drought and high intensity events of cold stress presented during an event “El Niño” in 2016 and 2017 would made migrate a relationship normally in balance and without detrimental effect between *Fusarium* spp. and the regional variety Simijaca (var. Simijaca) to detrimental one condition causing disease, this is supported by the fact that the sudden epidemic of stalk rot in the Ubaté valley was not reported in the zone in at least 30 years despite *Fusarium* spp. is recognized importance as corn pathogens around

the world and therefore would be considered an emergent disease in Colombia associated with higher thermic amplitude in the zone and climatic change.

Different to temperate zones production where corn is sown and exposed to continuously increase in temperature from spring to summer, in the cold tropic the temperature condition is homogenous and constant along year so that corn stalk rot in tropics is developed just when there is a misbalance between plant and their environment (Phytobiome) (Hawkes and Connor, 2017). In this sense a righter form to predict the vulnerability of this and others corn varieties adapted to cold tropic climate zone production against stalk rot caused by *Fusarium* spp. must include their exposition to drought and cold so that breeding effort be consistent with high yield and low lodging under field conditions.

Plants possess wide defense mechanism against pathogenic fungi that includes low weight compounds that inhibit fungus like benzoxazinoides (Osbourn, 1999). Few *Fusarium* species can be detoxify benzoxazinoides being *F. verticillioides*, *F. subglutinans* y *F. graminearum* the most tolerant (Glenn et al. 2001). A limited species number of *Fusarium* have shown the capacity to detoxify benzoxazinoides and most have host associations with corn (Bacon et al. 2008), in this work *F. subglutinans* y *F. graminearum* was probed metabolized 2-benzoxazolinone so that is probably that *F. subglutinans* y *F. graminearum* have a host association with corn of the regional variety Simijaca too.

Due in corn benzoxazinoides have the major absolute concentration during the first 6-8 days after germination (Klun and Robinson, 1969) is probably that kept corn crop residues in the soil favor seed germination due early seed colonization by *F. graminearum* (FGSC) y *F. subglutinans* (FFSC). In this work the crop stand establishment was higher under corn monoculture scheme where crop residues were left (68,5%) which is in contrast with considerable reduction on seed germination of the regional variety Simijaca exposed at the same heat treatments here evaluated but under laboratory conditions where a gradual diminution on severity index in the seed and frequency of isolation of *Fusarium* spp. were detected (Piñeros-Guerrero et al. 2019).

In the field higher plant height and stem diameter were obtained under crop rotation scheme, intermediate when crop residues are removed and the lowest when are kept it. Yates et al. (1997) report a light but significative increase on plant height and stem diameter on corn plants inoculated with *F. verticillioides* (FFSC) 28 days after sown under growth chamber. The above contrast with height and stem diameter behavior observed in the Ubate valley, since in the scenario with the lowest amount of inoculum (crop rotation) higher height and stem diameter were obtained. It seems that association between Simijaca corn (var. Simijaca) and *Fusarium* spp. has an energetic cost for the plant, quantifiable by means of the height and stem diameter, so that benefits on growth due *Fusarium* spp. on early development stages as reported Yates et al. (1997) are transient.

With regard to parameters yield, crop rotation had a negative effect on the crop *fitness*, reducing to the middle the ear number per plant despite that highest height and stem diameter values were obtained in this scheme. In the corn monoculture scheme, where crop residues were removed or not, had double of production highlighting the importance of association of corn of the regional variety Simijaca (var. Simijaca) with *F. graminearum* y *F. subglutinans* in the Ubate valley. Individual thermal seeds treatments or planning crop sequences with residues removal had not significant effect on corn lodging. However, the joint implementation of crop rotation and seeds thermal treatments by means of dry heat at 50°C and 60°C generated net reductions of 54% and 23% respectively on lodging.

In this sense, the long-term crop rotation, in order to reduce the inoculum potential of *Fusarium* spp. seems not be a desirable management measure in terms of yield since, although in effect lower incidences of corn Stalk Rot and lodging are obtained when crop rotation is implemented with respect to corn monoculture with or without removal of corn crop residues, there is a reduction on the crop

fitness and yield despite that highest height and stem diameter values were obtained under crop rotation.

In this study the increase of ear number per plant and their weight under the monoculture scheme can be explained due stalk rot, since corn plants with stalk rotted present 10-19% more grains than adjacent healthy plants without any evident stress symptom or disease (Dodd, 1980b), highlighting the importance of nutrient cycle since an important number of sugars is liberated and translocate from stalk to ears. Furthermore, chemical and textural analyses from experimental plots in Simijaca were not associated with these growth and yield modifications.

Due that weight of 10 ears between crop residues management ($P=0,122$) and seed treatments ($P=0,22$) did not show statistical difference and that crop residues schemes are not comparable in the ear number and weight due own dynamics of establishment and lodging, differences found on yield are due to the ear number per plant at harvest. Results on corn growth and yield show changes associated to seeds thermal treatments and crop residues management present in the soil, that are not evident from sowing but are reflected on yield and growth parameters.

Although has been known *Fusarium* inoculum diminution present in seed by means heat treatments and their implications on germination and plant vigor (Bennett and Colyer, 2010; Clear et al. 2002; Coutinho et al. 2007; Daniels, 1983) to our knowledge few studies evaluate growth and yield parameters of seeds treated with heat under field conditions, in the present study it was shown that kept corn crop residues on the soil surface stimulates germination and establishment, which translates into greater yield potential. This suggest re-evaluating the way non-mechanization or tillage practices are carried out since, although leave corn crop residues has contributed to disease outbreaks (Keller et al. 2011), it is possible that the association between *F. graminearum* and *F. subglutinans* and corn will be indeed beneficial to the crop.

However, the management of the inoculum potential through the planning of the crop residues management and heat seeds treatments is likely to be appropriate and not the complete elimination or accumulation of the inoculum potential and such decision must consider the ecological and the climatic context where corn grows (phytobiome) as mentioned by Hawks and Connor (2017). Managing the inoculum potential on corn crops residues and seed would allow higher yields as long as these measures are implemented together.

The obtained results show a cost-benefit relationship between the corn of the regional variety Simijaca and *F. graminearum* / *F. subglutinans* throughout the entire crop cycle, highlighting the importance of this association for this variety of corn adapted to the Andean cold climate zones production in the Colombian tropic. Despite the extensive literature on pasture endophytes where their benefit to plant performance has been understood through increased plant vigor, pest resistances and stress tolerance (Funk et al. 1994), few investigations have documented the impact of fungi on the growth, development and yield of field crops (Yates et al., 1997). In the case of cold climate corn, the results obtained in this work could be just one example of the benefit provided by *Fusarium* spp. under cold tropic conditions to Simijaca corn variety (var. Simijaca).

Although additional studies are necessary to delve into cold climate corn stalk rot and its management, the comprehensive evaluation of the disease and of crop growth and yield addressed in this study made it possible to demonstrate that crop rotation with species other than grasses for periods of more than two years is not desirable in terms of yield for the study area and the management of corn crop residues in the short term along with disinfection of corn seed through heat treatments can contribute to crop yield and disease control.

Nevertheless, the relevance and pertinence of such management measures requires the analyses of sowing date and the evaluation of the risk of disease occurrence that allow deciding whether such management measures are necessary. Finally, the chemical treatment implemented by the farmers in the area showed a reduction on seed germination, the number and weight of ears, the number of ears per plant and an increase in the incidence of stalk rot, therefore it cannot be considered as a recommended treatment for the management of the disease.

V. CONCLUSIONS

This work discusses the emergence of *Fusarium* stalk rot as an economically important disease in corn crops (var. Simijaca) adapted to cold tropic conditions of Colombia, due the reduction on precipitation levels and higher thermic amplitude with reduction on minimal temperature framed on an “El Niño” episode during 2017. The study found that the principal inoculum sources of *Fusarium* spp. are the corn crop residues and seed. Practices to reduce the inoculum potential of both sources had a positive effect on reducing stalk rot incidence and lodging, particularly when heat seed treatment was implemented with crop rotation. However, on yield terms, crop rotation reduced the ear number per plant, highlighting the importance of association of the *F. graminearum* and *F. subglutinans* with corn of the regional variety Simijaca under cold the Ubaté Valley conditions. Future efforts on stalk rot breeding programs on corn varieties adapted to the cold tropic conditions must considerer their evaluation under cold and drought stresses conditions, so that breeding effort be consistent with high yield and low lodging under field conditions. Finally, the development of disease risk models for corn stalk rot in cold tropic would contribute to more effective measures of control.

ACKNOWLEDGMENTS

The authors would like to thank the project "Improving the competitiveness of bean and corn crops in the regions of Ubate and Guavio in the department of Cundinamarca" within the “Corredor tecnológico agroindustrial Bogota-Cundinamarca CTA-2” which funded this research with resources from the General System of Royalties, from the Secretary of Science and Technology of the Department of Cundinamarca and the District Secretary of Economic Development of Bogotá.

Conflict of interest statement

The authors declare that there is no conflict of interests for the publication of this article. Author’s contributions GMA conducted the research and investigation process and wrote the original draft. GMA, GLM, and SGC formulated the overarching research goals and aims, wrote, reviewed and edited the manuscript. SGC verified the overall replication/reproducibility of results. SMM conducted the statical analyses. GLM and SGC obtained the financial support for the project leading to this publication. All authors reviewed the manuscript.

REFERENCES

1. Bacon, C. W., Glenn, A. E., y Yates, I. E. (2008). *Fusarium verticillioides*: Managing the endophytic association with maize for reduced Fumonisin accumulation. *Toxin Reviews*, 27 (3-4), 411–446. doi:10.1080/15569540802497889.
2. Bennett, R.S. y P.D. Colyer. (2010). Dry heat and hot water treatments for disinfecting cotton seed of *Fusarium oxysporum* f. sp. *vasinfectum*. *Plant Disease*. 94, 1469-1475. Doi: 10.1094/PDIS-01-10-0052
3. Blandino, M., Reyneri, A., Colombari, G., y Pietri, A. (2009). Comparison of integrated field programmes for the reduction of fumonisin contamination in maize kernels. *Fields Crops Research*, 111, 284–289. <https://doi.org/10.1016/j.fcr.2009.01.004>

4. Borja, I., Sharma, P., Krekling, T., y Lonneborg, A. (1995). Cytopathological response in roots of *Picea abies* seedlings infected with *Pythium dimorphum*. *Phytopathology*, 85:495- 501
5. Broders, K. D., Lipps, P. E., Paul, P. A., y Dorrance, A. E. (2007). Evaluation of *Fusarium graminearum* associated with corn and soybean seed and seedling disease in Ohio. *Plant Disease*, 91(21), 1155–1160. <https://doi.org/10.1094/PDIS-91-9-1155>
6. Buritica, P. (1999). Directorio de Patógenos y enfermedades de las plantas de importancia económica en Colombia. Instituto Colombiano Agropecuario (ICA). Bogotá, Colombia. 331 pp.
7. CIAT and CIMMYT. (2019). Maíz para Colombia Visión 2030. Colombia: CIAT and CIMMYT publishing, 110 pp.
8. Clear, R.M., Patrick, S.K., Wallis, R. y Turkington, T.K. (2002). Effect of dry heat treatment on seed-borne *Fusarium graminearum* and other cereal pathogens. *Plant Pathology*, 24, 489-498. Doi: 10.1080/07060660209507038
9. Cotten, T. K., y Munkvold, G. P. (2007). Survival of *Fusarium moniliforme*, *F. proliferatum*, and *F. subglutinans* in Maize Stalk Residue. *Phytopathology*, 88(6), 550–555. <https://doi.org/10.1094/phyto.1998.88.6.550>
10. Coutinho, W., R. Silva, M. Vieira, C. Machado, y Machado. J. (2007). Qualidade sanitária e fisiológica de sementes de milho submetidas a termoterapia e condicionamento fisiológico. *Fitopatologia Brasileira*. 32, 458- 464. Doi: 10.1590/S0100- 41582007000600002
11. Daniels BA. (1983). Elimination of *Fusarium moniliforme* from corn seed. *Plant Disease*, 67: 609-611.
12. Dodd, J. L. (1980a). The Role of Plant Stresses in Development of Corn Stalk Rots. *Plant Disease*, 64(6), 533–537
13. Dodd, J.L. (1980b). Grain silk size and predisposition of *Zea mays* to stalk rot. *Phytopathology*, 70: 534-535
14. Drayton, F. L. (1929). Bulb growing in Holland and its relation to disease control. *Scientia Agricola*, 9:494-50
15. Duncan, K. E., y Howard, R. J. (2010). Biology of maize kernel infection by *Fusarium verticillioides*. *Molecular Plant-Microbe Interactions*: MPMI, 23(1), 6–16. doi:10.1094/MPMI-23-1-0006
16. Funk, C. R., Belanger, F. C., y Murphy, J. A. (1994). Role of endophytes in grasses used for turf and soil conservation. 201-209. in: Biotechnology of Endophytic Fungi of Grasses. C. W. Bacon y J. F. White, Jr., eds. CRC Press, Boca Raton, Florida
17. Glenn, A. E., Hinton, D. M., Yates, I. E., y Bacon, C. W. (2001). Detoxification of corn antimicrobial compounds as the basis for isolating *Fusarium verticillioides* and some other *Fusarium* species from corn. *Applied and Environmental Microbiology*, 67 (7), 2973–2981. doi:10.1128/AEM.67.7.2973-2981.2001
18. Glenn, A., Gold, S., y Bacon, C. (2002). *Fdb1* and *Fdb2*, *Fusarium verticillioides* loci necessary for detoxification of preformed antimicrobials from corn. *Molecular Plant-Microbe Interactions*, 15, 91-101
19. Hawkes, C. V, and Connor, E. W. (2017). Translating Phytobiomes from Theory to Practice: Ecological and Evolutionary Considerations. *Phytobiomes*, 1(2), 57–69. doi:10.1094/PBIOMES-05-17-0019-RVW
20. Irizarry, I., y White, J. F. (2018). *Bacillus amyloliquefaciens* alters gene expression, ROS production and lignin synthesis in cotton seedling roots. *Journal of Applied Microbiology*, (July), 1–15. <https://doi.org/10.1111/jam.13744>
21. Keller, M.D., Thomason, W.E., Schmale III, D.G., (2011). The spread of a released clone of *Gibberella zeae* from different amounts of infested corn residue. *Plant Disease*. 95 (11), 1458–1464

22. Klun, J., y Robinson, J. (1969). Concentration of two 1,4-benzoxazinones in dent corn at various stages of development of the plant and its relation to resistance of the host plant to the European corn borer. *Journal of Economic Entomology*, 62, 214-220
23. Kuldau, G.A, y Yates, I.E. (2000). Evidence for *Fusarium* endophytes in cultivated and wild plants. In C.W Bacon, y J. White, Microbial Endophytes (pp. 85-117). New York: Marcel Dekker
24. Leslie JF and Summerell B. (2006). The *Fusarium* laboratory manual. USA: Blackwell publishing. Iowa, USA. 387 pp.
25. Ligarreto, G.A. (2017). Selección de semilla de maíz Simijaca. Universidad Nacional de Colombia.
26. Maldonado-Archila, G., Ligarreto-Moreno, G. and Gómez-Caro, S. (2022). Fusarium species that cause corn stalk rot in the Ubaté valley of Cundinamarca, Colombia. *Agronomía Colombiana*, 40(2), 237–248. <https://doi.org/10.15446/agron.colomb.v40n2.102465>
27. Machado, J.D.C., A. Machado, E.A. Pozza, C.F. Machado, y Zancan, W. (2013). Inoculum potential of *Fusarium verticillioides* and performance of maize seeds. *Tropical Plant Pathology*, 38(3), 213-217. Doi: 10.1590/S1982-56762013000300005
28. Manzo, S. K., y Claflin, L. E. (1984). Survival of *Fusarium moniliforme* hyphae and conidia in grain sorghum stalks. *Plant Disease*, 68: 866-867
29. Munkvold, G., Hellmich, R., y Showers, W. (1997). Reduced *Fusarium* ear rot and symptomless infection in kernels of maize genetically engineered for European corn borer resistance. *Phytopathology*, 87, 1071-107
30. Nguyen, T. T. X., Dehne, H. W., y Steiner, U. (2015). Histopathological assessment of the infection of maize leaves by *Fusarium graminearum*, *F. proliferatum*, and *F. verticillioides*. *Fungal Biology*, 120 (9), 1094–1104. doi: 10.1016/j.funbio.2016.05.013
31. Nguyen, T. T., Dehne, H., y Steiner, U. (2016). Maize leaf trichomes represent an entry point of infection for *Fusarium* species. *Fungal Biology*, 120 (8), 895–903. <https://doi.org/10.1016/j.funbio.2016.05.014>
32. Nyvall, R. F., y Kommedahl, T. (1970). Saprophytism and survival of *Fusarium moniliforme* in corn stalks. *Phytopathology*, 60, 1233-1235
33. Ooka, J., y Kommedahl, T. (1977). Wind and rain dispersal of *Fusarium moniliforme* in corn fields. *Phytopathology*, 67, 1023-1026
34. Osbourn, A. (1999). Antimicrobial phytoprotectants and fungal pathogens: a commentary. *Fungal Genetics and Biology*, 26, 163-168
35. Paliwal, R. L. (2016). Introducción al maíz y su importancia. FAO. <https://www.fao.org/3/x7650s/x7650s02.htm>
36. Piñeros-Guerrero, N., Maldonado-Archila, G. y Gómez-Caro, S. (2019). Effect of thermal and in vitro fungicide treatments on pathogens of the genus *Fusarium* associated with maize seeds. *Agronomía colombiana*, 37 (3): 228-238
37. Plantegenest, M., Le May, C., y Fabre, F. (2007). Landscape epidemiology of Plant disease. *Journal of The Royal Society Interface*, 4(16), 963–972. doi:10.1098/rsif.2007.1114
38. Pradhan Mitra, P., y Loqué, D. (2014). Histochemical Staining Secondary Cell Wall Elements. *Journal of Visualized Experiments*, 87(1), 1–11. doi:10.3791/51381
39. Prussin, A. J. (2013). Monitoring and predicting the Long-Distance Transport of *Fusarium graminearum*, Causal Agent of *Fusarium Head Blight* in Wheat and Barley. Virginia Polytechnic Institute and State University, 172 pp.
40. Ritchie, SW, Hanway, JJ and Benson, GO. (1996). How a Corn Plant Develops? Iowa State University Cooperative Extension Special Report No. 48. Ames, Iowa, USA
41. Saab, I., y Steve, B. (2006). Diagnosing Chilling and Flooding Injury to Corn Prior to Emergence. Pioneer Hi-Bred Int'l. Retrieved from https://www.pioneer.com/growingpoint/agronomy/library_corn/crop_injury/flooding_injury.js_p

42. Schmale, D., Shields, E., y Bergstrom, G. (2006). Nighttime spore deposition of the *Fusarium* head blight pathogen, *Gibberella zeae*, in rotational wheat fields. *Canadian Journal of Plant Pathology*, 28, 100-108.
43. Schulz, B., Remmert, A., Dammann, U., Aust, H., y Strack, D. (1999). The endophyte-host interaction: a balanced antagonism. *Mycological Research*, 103, 1275-1283.
44. Sumner, D. R., Doupnik, B., y Boosalis, M. G. (2003). Effects of Reduced Tillage and Multiple Cropping on Plant disease. *Annual Review of Phytopathology*, 19 (1), 167-187. <https://doi.org/10.1146/annurev.py.19.090181.001123>.
45. Vance, C., Kirk, T., y Sherwood, R. (1980). Lignification as a mechanism of disease resistance. *Annual Review of Phytopathology*, 18, 259-288.
46. Van Wyck, P., Scholtz, D., y Marasas, W. (1988). Protection of maize seedlings by *Fusarium moniliforme* against infection by *Fusarium graminearum* in the soil. *Plant and Soil*, 107, 251-25.
47. Wang C, Yang Q, Wang W, Li Y, Guo Y, Zhang D, Ma X, Song W, Zhao J. and Xu M. (2017). A transposon-directed epigenetic change in ZmCCT underlies quantitative resistance to *Gibberella* stalk rot in maize. *New Phytologist*. 215, 1503-1515.
48. Wicklow, D. T. (1988) Patterns of fungal association with maize kernels harvested in North Carolina. *Plant Disease*, 72: 113-115.
49. Windels, C., Windels, M., y Kommedahl, T. (1976). Association of *Fusarium* species with picnic beetles on corn ears. *Phytopathology*, 66, 328-331.
50. Yang Q, Yin G, Guo Y, Zhang D, Chen S, and Xu M. (2010). A major QTL for resistance to *Gibberella* stalk rot in maize. *Theoretical and Applied Genetics*, 121, 673-687.
51. Yates, I. E., Bacon, C. W., y Hinton, D. M. (1997). Effects of Endophytic Infection by *Fusarium moniliforme* on Corn Growth and Cellular Morphology. *Plant Disease*, 81(7), 723- 728.



Scan to know paper details and
author's profile

Content Analysis of Design Language based on User Evaluation and Experience

Cai Yuanyuan, Mustaffa Halabi Bin Azahari & Khairun Nisa Binti Mustaffa Halabi

Xi'an University of Architecture and Technology

ABSTRACT

The aim of this paper is to explore the content and features of design language based on user evaluations and experiences. By analyzing user evaluations of different design language samples, the researcher examines the user understanding of different design languages in terms of visual design, interaction, usability, aesthetic appeal, and emotional effects, and explores user perceptions and preferences for design language. The paper uses an observational approach and focuses on user evaluations shared on authoritative product websites, extracting and summarizing important design language content from users' intuitive perceptions, usage experiences, and emotional effects. The results show that design language has significant influence on consumers in 12 main thematic features, which are increasingly important to modern consumers in design content. These 12 themes can provide reference for the development and application of design language, and offer guidance for enhancing user experience.

Keywords: user evaluations; design language; the content of the design language.

Classification: LCC: QA76.9.H85

Language: English



Great Britain
Journals Press

LJP Copyright ID: 925694
Print ISSN: 2631-8490
Online ISSN: 2631-8504

London Journal of Research in Science: Natural and Formal

Volume 23 | Issue 9 | Compilation 1.0



© 2023 Cai Yuanyuan, Mustaffa Halabi Bin Azahari & Khairun Nisa Binti Mustaffa Halabi. This is a research/review paper, distributed under the terms of the Creative Commons Attribution-Noncommercial 4.0 Unported License <http://creativecommons.org/licenses/by-nc/4.0/>, permitting all noncommercial use, distribution, and reproduction in any medium, provided the original work is properly cited.

Content Analysis of Design Language based on User Evaluation and Experience

Cai Yuanyuan ^α, Mustaffa Halabi Bin Azahari ^σ & Khairun Nisa Binti Mustaffa Halabi ^ρ

ABSTRACT

The aim of this paper is to explore the content and features of design language based on user evaluations and experiences. By analyzing user evaluations of different design language samples, the researcher examines the user understanding of different design languages in terms of visual design, interaction, usability, aesthetic appeal, and emotional effects, and explores user perceptions and preferences for design language. The paper uses an observational approach and focuses on user evaluations shared on authoritative product websites, extracting and summarizing important design language content from users' intuitive perceptions, usage experiences, and emotional effects. The results show that design language has significant influence on consumers in 12 main thematic features, which are increasingly important to modern consumers in design content. These 12 themes can provide reference for the development and application of design language, and offer guidance for enhancing user experience.

Keywords: user evaluations; design language; the content of the design language.

Author α: Xi'an University of Architecture and Technology.

σ ρ: City University of Malaysia Beilin, Xi'An, China, 710064.

I. DESIGN LANGUAGE

There are many languages that are available around us which include verbal, written, visual, art, design, music and many more to mention. It becomes very fundamental in daily human lives. The legend of the Tower of Babel highlights the importance of communication and language in human endeavors. Without a shared language, people are unable to understand each other, and cooperation becomes difficult if not impossible. The language system is very important in human society, and the role that it plays in enabling us to communicate, cooperate, and achieve our goals.

Similarly, in the field of design, whether it is to meet requirements or solve problems, the design language is the origin of problem solving. In the aspect of branding and product design, design language has been the subject of extensive research in recent years. It reveals a growing interest in understanding the key elements that make up a successful design language, as well as the impact that design language can have on user experience and brand perception. Dong and Chen (2018) found that a consistent and coherent design language could enhance the perceived personality of a brand. Lee and Jang (2019) explored that a coherent and consistent design language could improve user satisfaction and usability, by providing users with a clear and intuitive interface. The study suggested that design language could play a crucial role in creating a positive user experience. Wang (2020) focused on the use of design language in cross-cultural contexts, and highlighted the importance of considering cultural factors when designing a design language. A well-defined and coherent design language can enhance brand personality, improve usability, and create a positive user experience. These topics are

typical external manifestations of the design language, but the content and functions of the design language are more than that.

II. HOW TO THINK ABOUT DESIGN LANGUAGE

The process of design realization will produce various forms to truthfully express the results of problem solving, which is an essential basic form of design thought in the process of realization -design language. Design language structure is a comprehensive language structure, which contains the language of science and technology as well as the language of art. Auguste Enderpointed out: "We are at a new beginning of art development. This art is an unprecedented plastic art" (as cited in Ma, C. 2008, p.108). Masayuki Kurokawa, a representative of the new era of Japanese architecture and industrial design, has been exploring the "meaning" of objects in his design. He believes that actual objects are only appearances in design, and the unmeasurable philosophy and ideas carried by objects are "meanings". In his view, what designers should explore is not "future and completely new design", but "genuine and profound design". Therefore, many of his works had undergone in-depth research on human behavior and feelings, and he had brought many designs beyond time to the world. Therefore, the language of design should be carefully crafted and thoughtfully executed to ensure that it effectively communicates the desired message and achieves the intended goals of the design, and it is important to evoke the desired emotions or reactions from the viewers or users.

This goes back to user-centered design, paying attention to the needs of the users and improving their experience. The study conducted by Cooper et al. (2007) involves users in the design process, conducting user research, and testing prototypes with users, in particular consider factors such as the user's age, gender, culture, and abilities (Dumas & Redish, 2011). The user becomes the target to be directly observed and participate in the design. According to Norman (2013), designers should use simple and clear language in their designs to ensure that users can easily understand and navigate through the product. This involves using common words and avoiding technical jargon. Additionally, designers should use visual cues and symbols to communicate ideas and concepts. In a study conducted by Goodwin (2009), it was found that designing for the user involves using a language that is familiar and meaningful to the user.

These are all effective studies and theories, but in the face of China's vast market, with a huge base of products and consumers, how to quickly understand and master the user information and transform it into guiding elements that young designers can refer to and use in design activities. This is the research direction of the design language in this paper.

III. RESEARCH METHOD

3.1 Data sources

Psychology believes that observation is an active form of people's direct understanding of real objects, and it is a purposeful and planned perception. This article starts with the observation method. It has a clear research theme, defined observation object and data collection method but does not have any preconceived limitations for the design problem. Therefore, the structure is open, and the environment is natural, which can fully reflect the fuzzy, personalized, and dynamic characteristics of user design needs (Zhu, J. 2017), and maximizes the openness of researchers to obtain information. Such a research foundation is solid and extensive.

The researcher took the user evaluation published on the product purchase website as the data samples and selects Taobao websites to collect relevant data. Taobao, founded by Alibaba Group in May 2003, is

a large online retail and business circle in the Asia Pacific region and a popular online shopping retail platform in China. It has nearly 500 million registered users and more than 60 million regular visitors every day. At the same time, the number of online goods per day has exceeded 800 million, with an average of 48000 goods sold per minute (Baidu Wikipedia, n.d.).

Taobao's user evaluation system is open, and very rich and extensive. The evaluation volume of well-known and popular products can reach hundreds or thousands. From the perspective of the seller, the user evaluation system is the performance of the reputation of Taobao stores but from the perspective of consumers, user evaluation is very important auxiliary decision-making information. Consumers need to check the evaluation of other users to judge the real information and use effect of goods to help them make decisions. In recent years, to improve the quality and richness of the evaluation and improve the decision-making value of evaluation to consumers, Taobao platform is constantly adjusting and upgrading the evaluation system. Among the important measures are: The more words of effective evaluation (at least 300 words), the better. Additional evaluation should be accompanied by more than 3 pictures. Other than that, the evaluation is multiple dimensions, from the quality of the product itself to the design style of the after-sales service and logistics. The researcher believes that this is a favorable data source to obtain the relationship between the consumers/users and design language.

3.2 Inclusion criterion

Because the user evaluation information of the network platform is cross regional and long-term display, the researcher was not worried about the short time span of observation, narrow information, and other issues. So, the observation research plan was implemented in two weeks and the information collection and sorting was completed at same time. The focus of the plan was how to select the design product as the observation sample to be more persuasive. The researcher had set several selection criteria:

- Classic design products in history are still being produced and used today (e.g., Barcelona chair, PH lamp, Beetle car, etc.)
- Award winning products in the international design competition (e.g., Red Dot Award, IF Award, Good Design Award, etc.)
- Representative products of famous brands (such as Apple, Muji, Dyson, ±0 Naoto, B&O, etc.)
- New popular design products (such as balance cars, VR glasses, fashionable small household appliances, etc.)
- These typical samples were selected after making sure that each sample had sufficient user evaluation (>100) on the network platform.

When the product meets the above selection criteria, the researcher will enter the product page, confirm that the various information meets the standards again (see figure1), and then enter the user evaluation page, quickly browse each user reviews (see figure2), find useful information, and then record them.

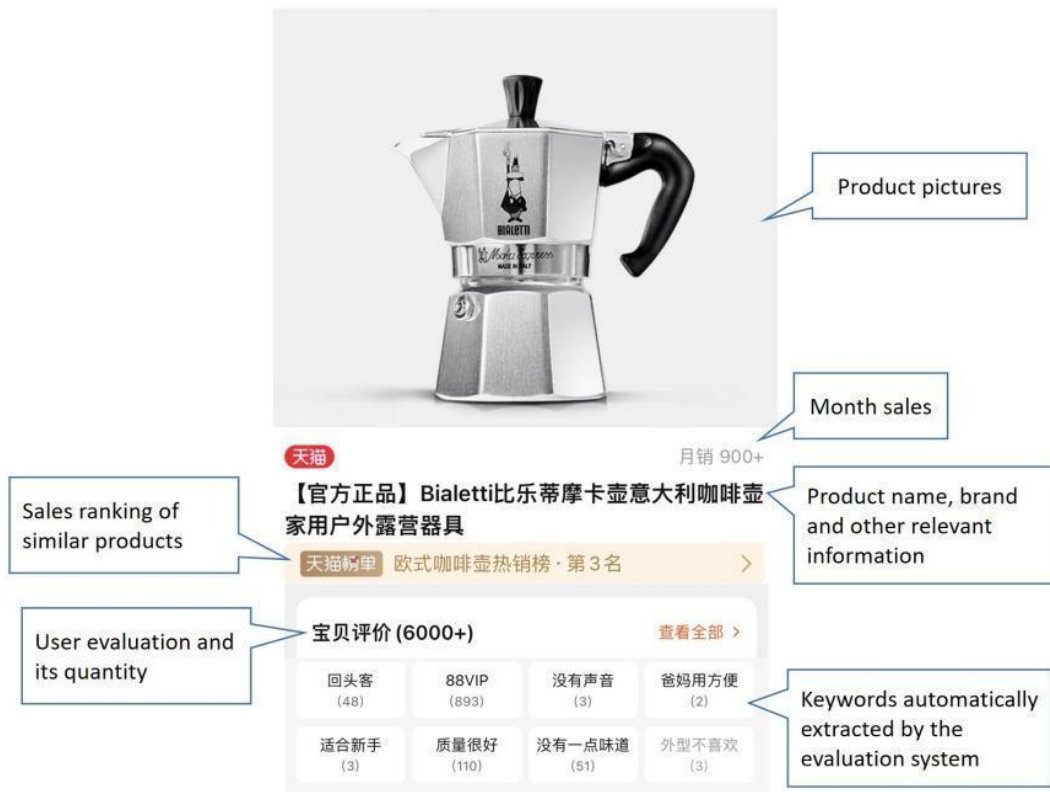


Figure 1: Selection of Design Samples




Figure 2: The details of user reviews for each product

3.3 Data analysis

The user's product evaluation is often a loose oral mode. The researcher read the information according to a certain logical order, from the appearance to the interior, from the whole to the details, from the first impression to the emotional summary, that are, look-and-feel, touch, price, performance, experience, brand, and emotional association. The evaluation keywords were ranked from high to low according to the frequency of these aspects.

Table 1: Information collection form for each survey sample

No.	Product	User evaluation		
		High-frequency words	Occasional-words	Quantity
		classic, smooth and stable, troublesome disassembly and cleaning, very feeling, beautiful, design, compact and beautiful	easy to use, aluminum products need maintenance, feelings and ornaments	300+

User evaluation interface can show initial messages and additional messages. Initial messages gave the overall sense of the product and the first feeling of the user; The additional messages highlighted the experience using the product in the later stage and giving feedback after using it for a period, or even put forward various suggestions. The researcher clicked on each evaluation and recorded the key points while reading, then recorded the content that had been put forward many times by different users in the "high-frequency words of user evaluation", and recorded the product evaluation points put forward by individual users in the "occasional words of user evaluation", to accumulate the products with typical design language characteristics that were widely concerned and used by users, and what aspects of users' design language concerns.

According to the above sample selection criteria, screen product pages and browse user reviews one by one, then record key words and sentences, and finally complete the survey of a total of 50 design samples (table 1 is one of the example). In the users product evaluation statements, classify the records, analyze the high-frequency words and the meaning behind the statements evaluated of each product sample, that is, the design semantic content that the public pays attention to, and draw key research themes from them.

3.3 Discussion & Results

The original data obtained by the observation method was decomposed and compared and then reassembled in a new way. Here, the original data were the high-frequency statements of user evaluation recorded in the observation process. They represented the design content that the public pay most attention to and feel most deeply when purchasing and using products. For each typical product design, the researcher classified the statements with the same or similar meanings in the user evaluation after recorded, and then reorganized them into the expression of design terms. In this way, all user evaluation contents were sorted and classified into the following 12 themes:

3.3.1 Needs

In the evaluation statement of the product, 90% of the users expressed that "it fully meets my requirements", "is what I want", "is very satisfied", and "has not been disappointed", "have wanted the product for a long time", and occasionally expressed that "can't wait to open or try it", which fully reflected that meeting the needs was one of the important design contents for public concern especially product design. The satisfaction of needs was one of the important psychological contents in their use design, experience design and feedback design.

3.3.2 Expectations

On the basis of meeting the needs, 50% of the users put forward the design and use of the product: "it is better than expected", "it is very useful", "beyond expectations", "very amazing", "has been expected long time", and "wants to scream when seeing the real object", which showed that the design also provided users with content beyond their expectations. Just like Maslow's hierarchy of needs theory, people's needs manifest differently at different stages, and the objects and services provided by the design should also be hierarchical. Especially in today's experiential consumption era, not limited to basic needs, meeting consumers' expectations and providing additional surprises is the competitiveness of design.

3.3.3 Visual intuition

In the evaluation statement of the product, almost all users mentioned their first impressions about the product. First is visual feeling: good-looking, lovely, textured, tasteful, special color, high face value, "fall in love at a glance", "looking cool", stylish, retro, and "the curve gives a sense of design". These descriptions can be said to be the beginning of attracting consumers, allowing consumers to activate their intuition and experience. This is a very important early link that affects the relationship between the public and design.

3.3.4 Comparison

In the user evaluation statement of the sample product, 30% of the users mentioned that the product was comparable with the competing products of the same kind. For example, "this is my choice after comparison", "I regret that I bought it late", "Soft natural wind more comfortable than traditional air conditioning", "dries faster than ordinary hair dryers", "does not hurt my hair", and "is very soft". Also, they expressed the comparison between the existing product and the previous product, such as "it is easier to use than previous products"; It also describes how can get a better experience after using the product themselves, such as "Homemade coffee is much better than Starbucks", "which saves a lot of time after use". Users naturally compare the product they are using with similar products they have used in the past. These comparisons may be unconscious, but they have a significant impact on the user's experience and satisfaction with the product. Comparison is a natural and necessary cognitive and decision-making process, so designers and researchers need to consider the user's comparative psychology to express the consistency or difference of the new design through the design language.

3.3.5 Appearance operation

Next, 90% of users evaluated the appearance operation of the products: "the details are in place", "the operation is simple", "the installation is convenient", "the three in one function", "the disassembly is simple", "the cleaning is easy", "the push-buttons are responsive", "the fully automatic operation and easy to learn"... which is an indispensable and important language of design with use function. Design can inform users of the safety and convenience of operations through its appearance, such as clear labeling and marking, use easily understood language and images, provide appropriate feedback and prompts, use intuitive interface design. This is the basis for enhancing the user experience and design feeling.

3.3.6 Sense of texture

In addition to the design content of the appearance operation, the user also expressed the experience of the design materials, sometimes just a general receptive evaluation: good texture, comfortable, high-end, durable; Sometimes specific evaluation of the material types to express their likes or dissatisfaction: solid wood, plastic, glass, titanium steel, stainless steel, aluminum alloy, piano paint, frosted texture, medical Seiko bearing steel, "The surface recycled aluminum (Apple earphone)", "easy to be stained with oil when cleaning plastic", "very special to use glass to transmit sound"; Individual users are also aware of the green materials: "the material is environmental friendly"... which all reflected the public's are increasingly comprehensive and professional in focusing on design. The selection of different materials has a direct impact on the user's experience of using the product, particularly for things like handles, buttons, control interfaces, and product surfaces. Additionally, it also affects the user's psychological evaluation of the product; the use of high-quality materials and exquisite craftsmanship can make users feel that the product is more high-end, delicate, and of better quality. Finally, the choice of materials also directly impacts the product's adaptability and durability in different environments. Therefore, the design language related to materials is also an essential aspect of the design process.

3.3.7 Technical performance

Another part of users design evaluation expressed their understanding of the inherent technicality and design concept of the product: "program intelligence", "acceptable working noise, which represents strong power", "low power consumption", "good battery life", "low energy consumption", "cost-effective", "humanized design", "classic design", "clever design", "suspended lyrics sound, so that music can be seen", "audio-visual sharing", "the sound quality is comfortable and clean", "the charm of music is better felt", "the aesthetic design has a good sense of fluid (B&O stereo)", "the design conforms to the principles of ergonomics (Barcelona chair)"... These design evaluations showed that the public's understanding of design has shifted from appearance to technical performance, which is one of the important charms of modern design. This highlights an important characteristic of modern design - the external appearance of a design must match its internal technological principles and structural processes. Therefore, the fundamental principles of design language should also be consistent with the technical core - practical and reasonable in reality.

3.3.8 Memory and association

In the user evaluation, there is still a considerable part of the impressive content. In addition to objectively describing the impression of the product design, their feelings also affect more memories and associations. For example, after experiencing the Apple headset, they concluded that its design was a continuation of Apple brand design... In addition, "The product is full of memories of me and my boyfriend"; "The product reminds me of the fireplace in northern Europe", "the scene of being in bed in winter", "I look forward to witnessing the ten and twenty years of a family together with the product"... These very sentimental comments show the irrational side of design language. The evocation of memories and associations is a comprehensive effect of design language, which is achieved through specific forms, colors, materials, functions, and other aspects. However, the reflection on this theme and how to resonate with users needs to be explicitly presented in the content of design language.

3.3.9 Emotional trigger

Most users' evaluation of the product experience always expressed by emotions: "too much like it", "create a romantic feeling", "use is full of ritual", "like so much that I cannot bear to part with it", "with a great atmosphere", "the use process is very healing", "strong sense of happiness", "the color that strikes the soul", "rose red has the feeling of first love"... Behind these sentences, it seems that we can

feel the most vivid and touching part the public triggered by the design. Design can stimulate human emotions in a way that makes people more likely to establish a connection with a product or service, resulting in deeper levels of engagement and loyalty. The current direction of design is focused on how design language can evoke emotions and trigger people's intuitive thinking, which has gradually evolved over the course of human evolution due to the need to adapt to complex environments and social contexts. This type of intuitive thinking is also manifested as people's curiosity, creativity, and imagination. Designers aim to understand and leverage the characteristics of human intuitive thinking to create designs, products, and marketing activities that are more appealing and influential.

3.3.10 Cultural characteristics

Some users gave their own definitions of product design style: Italian style (Mocha pot), Japanese style, Nordic style, simplicity, modern retro, British style... The public has a certain basic understanding under the influence of design trends. In today's information society and era of material prosperity, consumers can understand and appreciate different design styles through visual media, shopping experiences, personal preferences and values, as well as education and cultural backgrounds. The development of design language needs to consider these factors to meet user needs, and reverse operation of these contents has also contributed to distinctive design language styles.

3.3.11 Experience process

In addition to the evaluation of the product itself, users also extended the evaluation content to the entire service system: "after-sales service is patient and professional", "delivery is fast", "packaging is safe/tight/high-grade", "small gifts are given carefully", "the included product bracket is convenient for storage"; The overall design experience is sublimated by users into a feeling for life: "every day when use it is a kind of enjoyment", "every night I want to wake up every morning and have a cup of strong coffee to start a beautiful day"... These cognitive contents not only need to be conveyed through the language of design itself, but also need many intangible and social service design languages.

3.3.12 Impression and feedback

After the design experience, users also gave positive feedback, such as: "will recommend", "strongly recommend", "tell my friends around me", "it is suitable as a gift", "the first choice for gifts", "already become a loyal user", "will always choose this brand of products", "will not use other brands", "classic brands are worth having". This is a very important aspect of building brand communication and loyalty through design language. Another users expressed that the positive impetus brought by having the product, which let users "love drinking water with it" and "children like brushing teeth by themselves", which is just the power of design because excellent design language makes users love and trust, and leads to a better life.

The above 12 key themes are the content of design language explored from consumers' attention and experience from observation survey.

IV. CONCLUSION

Due to the prevalent use of the internet and the features of the current consumption era, regular consumers are becoming increasingly aware and appreciative of design. Consequently, a multidimensional comprehension of design has surfaced, encompassing not solely its utilitarian features and usability, but also its experiential and affective facets, as well as its brand perception. Modern richness is an asset and challenges the design language. The content of design language should be established on a logical framework that contains fundamental elements and allows for development and innovation. This paper centers on the needs and expectations of current major consumers

regarding design language. It provides a detailed analysis of these requirements and arranges them into key themes using professional terminology, with the aim of guiding the design practice work. 12 themes are the basic framework of the design language content, and the specific operation of the design in each of them can be changed or even updated and broken through in different design fields.

REFERENCES

1. Nippert-Eng, C. (2010). The narrative turn and the possibilities for design studies. *Design Issues*, 26(3), 3-17.
2. Walter, A. (2011). *Designing for Emotion. A Book Apart*.
3. Nimkulrat, N., Ylirisku, S., & Hansson, H. (2016). Designing with narrative: Towards a discourse-centred approach to design. *International Journal of Design*, 10(3), 1-16.
4. Wheeler, A. (2017). *Designing Brand Identity*. John Wiley & Sons.
5. Nimkulrat, N., Fong, K., & Siang, T. (2016). Designing with narrative: Towards a discourse-centred approach to design. *Craft Research*, 7(2), 165-183.
6. Dong, H., & Chen, X. (2018). The Effect of Design Language on Brand Personality: An Empirical Study. *International Journal of Industrial Ergonomics*, 68, 41-49.
7. Lee, H., & Jang, Y. (2019). The Impact of Design Language on User Experience in Digital Products. *International Journal of Human-Computer Interaction*, 35(4-5), 376-387.
8. Wang, J., & Wang, D. (2020). Design Language in Cross-Cultural Product Design: A Study on Visual Elements. *International Journal of Design*, 14(1), 1-16.
9. Cooper, A., Reimann, R., & Cronin, D. (2007). *About Face 3.0: The Essentials of Interaction Design*. John Wiley & Sons.
10. Dumas, J. S., & Redish, J. C. (2011). *A Practical Guide to Usability Testing*. Intellect Books.
11. Goodwin, K. (2009). *Designing for the Digital Age: How to Create Human-Centered Products and Services*. John Wiley & Sons.
12. Norman, D. A. (2013). *The Design of Everyday Things*. Basic Books.
13. Ma, C. (2008). Philosophical exploration of design semantics. *Packaging World*, 13(6), 108-112.
14. Zhu, J. (2017). The application of observational research in furniture design user research. *Design and Communication*, (9), 21-22.